THE UTILIZATION OF BIODEGRADABLE MATERIALS FOR THE DELIVERY OF BIOACTIVE MOLECULES THAT PROMOTE CNS REGENERATION

ELAINE TAN YEN MEI

NATIONAL UNIVERSITY OF SINGAPORE

2005

THE UTILIZATION OF BIODEGRADABLE MATERIALS FOR THE DELIVERY OF BIOACTIVE MOLECULES THAT PROMOTE CNS REGENERATION

ELAINE TAN YEN MEI

(B.App.Sc.(Hons.), NTU)

A THESIS SUBMITTED

FOR THE DEGREE OF MASTER OF SCIENCE

GRADUATE PROGRAMME IN BIOENGINEERING

FACULTY OF MEDICINE

NATIONAL UNIVERSITY OF SINGAPORE

2005

ACKNOWLEDGEMENTS

I would like to take this opportunity to thank my supervisor, Dr Alan Lee Yiu Wah for his continuous support, guidance and encouragement throughout the course of this project. I am also grateful to Dr Alan for his time and resources committed for the completion of this project.

I would like to extend my gratitude to Dr Wang Chi Hwa for his helpful advice and for kindly allowing me the use of equipment in his laboratory.

I would like to thank the following members of Dr Alan's laboratory for their technical assistance and advice: Ms Janice Law, Dr Li Xinhua, Mr Yang Jia and Mr Lewis Ng.

My thanks also to Mr Naraharisetti Pavan Kumar, Mr Xie Jingwei and Mr Lin Rongyi from Dr Wang's laboratory for their invaluable advice on microsphere fabrication.

TABLE OF CONTENTS

	Page
Summary	iv
List of Tables	vi
List of Figures	vii
Chapter One: Introduction	
1.1. Spinal cord injury	1
1.1.1. Axonal regeneration in the injured spinal cord	3
1.1.2. Signal transduction in axonal regeneration	4
1.2. C3 transferase	7
1.2.1. Cellular uptake of C3 transferase	9
1.3. Protein drug delivery	11
1.3.1. Drug delivery to the spinal cord	11
1.3.2. Anatomical features of the spinal cord	12
1.3.3. Methods of protein drug delivery to the spinal cord	14
1.3.3.1. Intrathecal infusion	14
1.3.3.2. Intraparenchymal delivery	16
1.3.4. Delivery of C3 transferase to the spinal cord	17
1.4. Microencapsulation of protein drugs	19
1.4.1. Protein release characteristics	22
1.4.2. Methods to modulate release characteristics	25
1.4.3. Protein stability	27

1.5. Motivation and Objectives 28

Chapter Two: Materials and Methods

2.1. Materials 30

2.1.1. Solutions and reagents for purification of C3 transferase 30

2.1.2. Materials for microsphere preparation 31

2.2. Preparation of cDNA encoding recombinant C3 transferase 31

2.3. Purification of recombinant C3 transferase 33

2.4. Sodium dodecyl sulfate-polyacrylamide gel electrophoresis (SDS-PAGE) 35

2.4.1. Coomassie blue staining 35

2.4.2. Western blot 36

2.5. Protein quantification 36

2.6. Determination of C3-TAT cellular uptake efficiency 37

2.7. Determination of *in vivo* biochemical activity of C3-Tat 38

2.8. Preparation of microspheres 39

2.8.1. Polymer blending 39

2.9. Determination of morphology and internal microstructure of microspheres 40

2.10. Determination of microsphere size 40

2.11. Determination of microsphere encapsulation efficiency 40

2.12. *In vitro* release studies 41

2.13. Enzyme-linked immunosorbent assay (ELISA) 42

2.14. Determination of change in pH of release medium 43

2.15. *In vitro* degradation studies 43

2.16. Determination of enzymatic activity of C3-TAT released into release medium 44

Chapter Three: Results and Discussion

3.1. Purification of recombinant C3-Tat 47

3.2. Biological efficacy of purified recombinant C3-Tat 50

3.2.1. Cellular uptake of C3-Tat 50

3.2.2. *In vivo* biochemical activity of C3-Tat in cells 51

3.3. Microencapsulation of C3-Tat in PLGA microspheres

3.3.1. Physical characteristics of PLGA microspheres encapsulating C3-Tat 53

3.3.2. Protein release characteristics of C3-Tat microspheres 56

3.3.3. Changes in physical characteristics of C3-Tat microspheres during degradation *in vitro* 59

3.3.4. Bioactivity of released C3-Tat 68

3.4. Discussion 70

Chapter Four: Conclusions and Recommendations

4.1. Conclusions 75

4.2. Recommendations 76

References 77

SUMMARY

Growth inhibitory proteins limit axonal regeneration in the injured spinal cord and a common effector of many of these inhibitors is the Rho family of small GTPases. Activation of RhoA leads to growth cone collapse and neurite retraction. An enzyme from *Clostridium botulinum*, C3 transferase, has recently been shown to block RhoA function by ADP ribosylation of the effector domain, and this promotes regeneration of injured neurons. Current methods for the delivery of C3 are inefficient and suffer from various drawbacks that limit its clinical application. The aim of this work was to develop a microsphere-based controlled delivery system for cell-permeable C3 protein that can be implanted in the injured spinal cord. The approach of blending capped (hydrocarbon end groups) and uncapped (free acid end groups) poly(D,L-lactide-co-glycolide) (PLGA) to achieve the desired continuous release of C3 was investigated. A recombinant, chimeric C3 protein incorporating a protein transduction domain from Tat, was first purified, and its purity, efficacy of cellular uptake and *in vivo* biochemical activity was demonstrated. C3-Tat loaded microspheres were prepared by a w/o/w extraction-evaporation technique. The microspheres were prepared from pure uncapped and capped PLGA and blends of 70/30, 50/50 and 30/70 ratios of capped/uncapped PLGA. Mean diameter of the microspheres ranges from 74 to 85 μm, with high encapsulation efficiencies of more than 80%. *In vitro* incubation of the microspheres in a HEPES buffer was carried out to assess the release profile and degradation behaviour. The degradation rate of the microspheres can be controlled by the blending ratio of capped and uncapped PLGA. The release of C3-Tat from the microspheres was controlled by matrix erosion, where interconnected

channels facilitated diffusion of the protein from the matrix. It was demonstrated that the optimal blending ratio giving rise to microspheres fulfilling the requirement of continuous release for at least one month, was a 30/70 ratio of capped/uncapped PLGA. In this formulation, an average daily C3-Tat release of 3.0 ng/day/mg microspheres was observed for a period of one month. While this study has demonstrated the suitability of the release characteristics of the microspheres for our target application, the activity levels of released C3-Tat could not be accurately assessed, given the instability of the protein in the *in vitro* release conditions. 70% of the released C3-Tat on the first day of incubation was found to be active. At least 40% of C3-Tat biological activity was maintained in the 30/70 microspheres for 19 days. Further characterization of the C3-Tat microspheres in rodent models of spinal cord injury is necessary for more accurate assessment of its biological activity. This study demonstrates the feasibility of encapsulation of C3-Tat into PLGA microspheres to provide constant delivery of C3-Tat to the injured spinal cord.

LIST OF TABLES

		Page
1	Pathophysiology of spinal cord injury	2
2	Characteristics of microspheres	54
3	*In vitro* degradation kinetics of the microspheres	63

LIST OF FIGURES

		Page
1	Mechanism of ADP-ribosylation of RhoA by C3 transferase	8
2	Encapsulation of a protein into microspheres following a typical w/o/w emulsification technique	20
3	Chemical structure of PLGA	21
4	*In vitro* degradation of PLGA immersed in aqueous solution	23
5	Schematic representation of the purification process of recombinant C3-TAT	35
6	Standard curve obtained by measuring extent of ADP-ribosylation for given amounts of freshly purified C3-TAT	46
7	Schematic representation of the expression construct for C3-TAT	47
8	Schematic representation of the GST-TAT-HA-C3 fusion protein purified from *E.coli* cell lysates	48
9	SDS-PAGE gel stained with Coomassie blue showing protein samples from various steps in the GST purification process	49
10	Western blot of purified GST-TAT-HA-C3 and C3-TAT protein (after thrombin cleavage) probed with anti-HA and anti-rabbit-HRP antibodies.	49
11	Efficiency of purified C3-TAT uptake into NIH 3T3 fibroblast cells	51
12	Intracellular activity of purified C3-TAT	52

13	SEM images of representative microspheres prepared from 100/0, 70/30, 50/50, 30/70 and 0/100 capped/uncapped PLGA.	55
14	Release of C3-TAT from microspheres prepared from blends of capped and uncapped PLGA	57
15	Non-cumulative release of C3-TAT from 30/70 capped/uncapped PLGA microspheres incubated at 37°C in a HEPES buffer	59
16	Change in weight-average molecular weight of microspheres incubated at 37°C in HEPES buffer	62
17	Semilog plots of the normalized weight-average molecular weight versus time	63
18	Mass loss profile of microspheres incubated at 37°C in HEPES buffer	64
19	SEM images of microspheres prepared from (a) 100/0, (b) 70/30, (c) 50/50, (d) 30/70 and (e) 0/100 capped/uncapped PLGA, after incubation in HEPES buffer at 37°C	65
20	The internal pore structure of 30/70 microspheres after 7 days of incubation in HEPES buffer	68
21	Percentage of C3-TAT that remained active after release from 30/70 microspheres	69

CHAPTER ONE

INTRODUCTION

1.1. Spinal cord injury

Three phases of injury, acute, secondary and chronic (Table 1), can be identified upon trauma to the spinal cord [1, 2]. The extent of these injuries determines the severity of motor and sensory function impairment. Traditionally, medical care involves removal of bone, disc and ligament fragments to decompress the swollen cord. One of the first pharmacological treatments for spinal cord injury is the steroid methylprednisolone, which may act by decreasing swelling, inflammation and free radical accumulation. It is widely accepted that comprehensive treatment should be a sequence of different interventions implemented at different intervals after injury. Current research is focused on therapies which reduce tissue damage at the injury site, promote axonal regeneration, restore appropriate myelination to damaged and regenerating fibers and achieving appropriate synaptic connectivity.

Table 1: Pathophysiology of spinal cord injury.

Stages of injury	Features
Acute (from moment of injury to the first few days after injury**)**	• The initial mechanical damage of neural and other soft tissue, e.g. endothelial cells of vasculature resulting from the trauma, leading to cell death • Propagation of action potentials along axons is slowed or completely blocked (electrolytic shifts), leading to failure in normal neural function and spinal shock • Hemorrhage, localized edema, vasospasm • Compression of spinal cord occurs as a result of vertebral displacement.
Secondary (minutes to weeks after injury)	• Excitotoxicity occurs whereby glutamate floods out of axon tips due to cell lysis from mechanical injury. This overexcites neighbouring neurons, which in turn let in waves of calcium ions that trigger production of free radicals, killing otherwise undamaged neurons. • Excitotoxicity also affect oligodendrocytes (CNS myelin producing cells) which explains why unsevered axons become de-myelinated and therefore cannot conduct impulses • Apoptosis (cell suicide) of oligodendrocytes and neurons • Neutrophils and lymphocytes invade the spinal parenchyma and increase local concentrations of cytokines and chemokines
Chronic (days to years after injury)	• Ion channel expression levels and activation states are altered • Cyst forms, and continues to enlarge in a condition called syringomyelia • Severed axons exhibit regeneration and sprouting but grow no longer than 1 mm • Neural circuits altered due to change in inhibitory and excitatory impulses • Permanent hyperexcitability, resulting in chronic pain syndrome

1.1.1. Axonal regeneration in the injured spinal cord

At the injury site, neurons die by necrosis, apoptosis or a combination of both. Any surviving neurons may be temporarily incapacitated by metabolic and ionic changes in their environment. Axons which are severed immediately upon injury undergo little spontaneous regeneration. Wallerian degeneration occurs distal to an injury, and in some cases the axotomised neuron dies due to loss of target derived, retrogradely transported trophic factors. The regenerative failure of mature central nervous system (CNS) axons after injury is one of the major reasons for little functional recovery in patients.

It is now clear that adult CNS axons are not intrinsically incapable of regeneration. To understand this, mechanisms of axonal growth during embryonic development should first be considered. As the nervous system develops, newborn neurons extend axons and dendrites toward their appropriate targets. The task of locating the target falls on the growth cone, the motile tip of a growing axon or dendrite. The growing axon grows on a strongly permissive substrate containing growth promoting molecules such as laminin. In addition, specific patterns of distribution of attractive and repulsive guidance cues guide axons to their targets. In the early postnatal period after all the major CNS tracts are laid down, the mammalian CNS loses the ability both to regenerate axons and to reestablish functional synaptic contacts. Reasons for this include absence of growth promoting substrate molecules and neurotrophic factors which mediate cell survival and neurite outgrowth during development. In addition, resting concentrations of cAMP are lower, which makes the growth cone more sensitive to several growth inhibitory molecules. Hence the growth permissive CNS environment changes to a nonpermissive one in the

adult. This change may only partially occur in the peripheral nerves, since axons regenerate in adult peripheral nervous system after injury.

Strong correlation between the failure of CNS axon regeneration and the deposition of a glial scar at the injury site shows that one of the main barriers to regeneration after injury is the presence of axonal growth inhibitors in the glial scar including proteoglycans, tenascins, ephrins and semaphorin III [3, 4, 5]. Experiments [6] have also shown that axons failed to extend over oligodendrocytes and CNS myelin in culture. Several CNS myelin/oligodendrocyte derived axon growth inhibitory ligands have since been isolated, which includes nogo, myelin-associated glycoprotein (MAG) and oligodendrocyte-myelin glycoprotein (OMgp) [7, 8, 9].

1.1.2. Signal transduction in axonal regeneration

Binding of inhibitor molecules to their transmembrane receptors on growth cones regulate axon pathfinding in the developing embryo. In adult, similar inhibitory interactions probably mediate plasticity and stabilize established connections [10]. After CNS injury, inhibitory ligand expression is upregulated and interaction with their receptors located on axon growth cones cause growth cone collapse and account for failure of damaged axons to regenerate.

Axonal growth cones rely on actin rearrangements and microtubule assembly to drive growth and guidance. The Rho family of small GTPases regulates the actin cytoskeleton

in both neuronal and non-neuronal cells. The most widely expressed small GTPases of the Rho family are RhoA, Cdc42 and Rac1. Rho GTPases act as molecular switches to control signal transduction pathways that link membrane receptors to the cytoskeleton. They cycle between active (GTP-bound) and inactive (GDP-bound) states through the binding of guanine nucleotides. The cycling of Rho GTPases is regulated by either enzymes that enhance GTP-binding activity (guanine nucleotide exchange factors, GEF) or proteins that increase GTP hydrolysis (GTPase activating proteins, GAP). When GTP bound, Rho GTPases can interact with a series of intracellular effectors to reorganize the cytoskeleton in two ways, first, by regulating actin filament assembly and disassembly by controlling actin polymerization, branching, and depolymerisation and second, by directing actin-myosin dependent contractility to control the retrograde transport of f-actin within the growth cone. In neuronal cell lines, activation of RhoA stimulates actinomyosin contractility and stress fiber formation, resulting in growth cone collapse. The activation of Cdc42 and Rac1 leads to extension of filopodia and lamellipodia, respectively.

Recent studies have shown that GTPases in neurons are critical signaling mediators which link signaling pathways stimulated by myelin associated inhibitors-cell surface receptor interaction to the modulation of cytoskeletal dynamics in growth cones [11,12]. *In vitro* studies have demonstrated that inactivation of RhoA specifically, by application of a bacterial enzyme known as C3 transferase (C3), stimulates primary neurons to extend neurites on various growth inhibitory substrates including myelin, chondroitin sulphate proteoglycans (CSPG), MAG and Nogo [13, 14, 15]. This points to the

requirement of RhoA activation to produce the inhibitory activity of myelin-associated inhibitors. *In vivo*, the regeneration of retinal ganglion cells axons in the optic nerve can be stimulated by C3 application [13].

Another recent *in vivo* study has demonstrated the benefits of C3 treatment in spinal cord injury [16]. In the study, C3 was applied to the spinal cord of adult mice in which injury had been induced by a dorsal over-hemisection. Long distance regeneration of corticospinal axons for up to 12 mm from the lesion site was observed in the treated animals, in contrast with axonal retraction in buffer-treated control animals. To assess functional recovery, hind limb motor function was measured using a BBB locomotor rating scale. The C3 treated mice were walking with body weight support within 24 hours after spinal cord injury and initiation of treatment. One month after treatment, the mice were walking with hind limb-front limb coordination. The authors speculated that the early functional recovery within one day is unlikely to be the result of regenerating axons making new functional reconnections. It is possible that these rapid effects may be due to reduced tissue loss. Supporting this view are recent studies showing that inactivation of RhoA with C3 in ischemic CNS tissue inhibited apoptosis related protein activation in neurons and reduced cerebral infarct size [17,18]. The improvement of locomotion at the later stages was attributed to long distance regeneration of axons. This study indicates that C3 administration is a promising therapy for spinal cord injury.

1.2. C3 transferase

C3 transferase (C3) is an exoenzyme secreted by type C and D strains of the anaerobic bacterium *Clostridium botulinum* [19, 20]. C3 is a basic protein (pI ~ 9.13) of about 25 kDa. C3 specifically modifies RhoA, RhoB and RhoC proteins from the RhoGTPase family via a reaction known as ADP-ribosylation (Fig.1). The other Rho GTPase family proteins such as Rac1 and Cdc42 are very poor substrates for C3. This covalent modification of RhoA results in inhibition of RhoA dependent processes. The interference of RhoA function by C3 is likely due to several mechanisms. One of them involves the fact that in the resting state, RhoA is kept in inactive form in the cytoplasm by forming a complex with guanine dissociation inhibitor (GDI). It is believed that the translocation of RhoA from the cytoplasm to the plasma membrane is necessary for its activation. Interaction between RhoA and ERM-proteins (ezrin, radixin, moesin) at the membrane is suggested to release RhoA from the GDI complex and exposes RhoA to its GEF protein. ADP-ribosylated RhoA accumulates in the cytoplasm and the release from GDI is blocked. Accordingly, translocation and activation of RhoA will not occur. In order to inactivate RhoA signal transduction inside cells, the majority of RhoA must be modified. ADP-ribosylation of RhoA appears to affect a variety of cellular signal transduction processes, including control of smooth muscle contraction, cell adhesion, cellular proliferation and transcriptional activation. C3 has been found to be a valuable tool for elucidating the function of RhoA in biological systems.

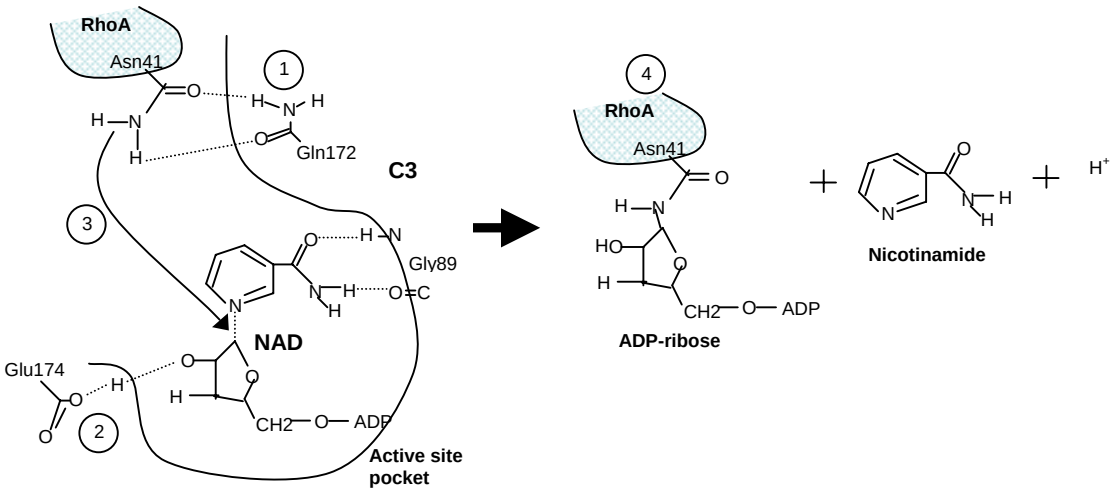

Fig. 1: Mechanism of ADP-ribosylation of RhoA by C3 transferase. (1) Glutamine residue at position 172 on C3 interacts with asparagine 41 of RhoA to position the acceptor amino acid precisely for the reaction. (2) Glutamic acid at position 174 of C3 interacts with O2' hydroxyl group of NAD+, to stabilize the oxocarbenium ion transition state of NAD+. (3) Amino group of asparagine 41 is a nucleophile which attacks the glycosidic bond in NAD+ and cleaves it. (4) C3 catalyses the transfer of the ADP ribose moiety of NAD+ to an asparagine residue at position 41 on RhoA.

1.2.1. Cellular uptake of C3 transferase

C3 transferase lacks the cell surface binding and transport component that is typically found for other families of bacterial toxins. Thus C3 is poorly taken up by cells since it does not efficiently cross the lipid bilayer of the plasma membrane. This was proposed to be the cause of failure of C3 to promote neurite outgrowth after corticospinal tract lesion in the adult rat [14]. In culture studies, invasive means including microinjection [19], trituration [20] or scrape loading [21] are necessary to allow C3 to penetrate neuronal cell bodies and promote neurite outgrowth. Most studies exploited the ability of C3 to enter cells by non-specific endocytosis when applied at rather high concentrations (30-150 μg/ml) and long incubation times (up to 24-48 hours). Various problems have been encountered in the use of invasive methods, including cellular damage, cellular toxicity and complex manipulation, all of which preclude their routine use *in vivo*.

One solution is to create a chimeric protein, comprising of fusion of a small transport peptide to C3, thus increasing the efficiency of C3 transduction across the cell membrane. The proof of concept for the transduction of proteins into cells was first described in 1988 independently by Green [22] and Frankel [23] with the discovery that the protein transduction domain (PTD) from the human immunodeficiency virus (HIV) Tat protein can cross cell membranes. The Tat protein is a transcription transactivator produced by the human immunodeficiency virus type 1 (HIV-1) at the early phase of infection, which plays a critical role in the expression and replication of the viral genome [24]. This 86 amino acid protein, which can be secreted from the infected cells, has the ability to enter uninfected cells and exert its activity upon the responsive genes. PTDs are small regions

of protein which have the ability to traverse biological membranes efficiently through a process termed protein transduction. Protein transduction occurs in a rapid, concentration-dependent fashion that appears to be independent of receptors and transporters but targets the lipid bilayer component of the cell membrane [25]. The ability of the Tat PTD to act as a carrier for heterologous proteins across cell membranes has been demonstrated through the intraperitoneal injection of a β-galactosidase protein fused to the Tat PTD [26]. This resulted in delivery of biologically active fusion protein to all tissues in mice. The membrane-permeating capability of Tat PTD in a receptorless fashion renders it a universal transduction system.

The commonly used PTD from Tat protein is the 11-amino acid peptide (Tyr-Gly-Arg-Lys-Lys-Arg-Arg-Gln-Arg-Arg-Arg). A fusion protein of Tat PTD and C3 has been reported to efficiently transduce across the plasma membrane of neurons to ADP-ribosylate and inactivate RhoA intracellularly [27]. The Tat-C3 fusion protein in that study also promoted significant neurite outgrowth on myelin substrates. It is clear that the fusion of Tat to C3 does not affect the biological activity of C3 *in vivo*, and is very effective in transducing cells.

1.3. Protein drug delivery

Modern biotechnology permits the large-scale production of highly purified proteins to be used as drugs in humans. In contrast to low molecular weight drugs, protein biopharmaceuticals are generally characterized by high clearances and short plasma half-lives as a result of rapid degradation by extracellular peptidases or significant receptor-mediated clearance, and poor passage through biological barriers due to their poor diffusivity and low partition coefficient. In addition, protein drugs often possess biological activity at multiple tissue sites throughout the body; therefore, systemic administration can lead to toxicity. Some of the problems that lead to low efficacy and unacceptable toxicity for many protein drugs may be overcome by matching a route of administration with an appropriate formulation, with the objective of obtaining an appropriate extent and time course of drug action while administering the drug as close as possible to its intended site of action.

1.3.1. Drug delivery to the spinal cord

Most of the molecules found to be beneficial to spinal cord regeneration, such as neurotrophic factors, and more recently, C3 transferase, are large proteins. In addition to the physicochemical properties of protein drugs described previously, the anatomy of the spinal cord poses a unique challenge for localized administration of such drugs to the site of injury in the spinal cord in biologically relevant amounts and for prolonged periods of time. Anatomical features of the spinal cord which have implications in spinal cord drug delivery will be discussed in the next section.

1.3.2. Anatomical features of the spinal cord

The spinal cord is part of the CNS and in humans, it is a 40 to 45 cm long cylinder of nervous tissue of approximately the same thickness as a little finger, extending from the lower end of the brain stem to the lower back. The consistency of the cord is soft and jellylike. It is protected by the vertebral column, which consists of 33 vertebrae. A circular space within each vertebra forms the spinal canal. The nerves linking the spinal cord and the periphery, which are responsible for sensory and motor innervation of the body other than the head and neck, are called spinal nerves. The spinal nerves exit the vertebral canal by way of spaces between adjacent vertebrae, known as intervertebral foramina.

The spinal cord is covered by three membranes, known as meninges. The outermost layer is the dura mater, a tough fibrous sheath closely applied to the inner layer of bone surrounding the spinal canal. Between the dura and the bone is the epidural space, which normally contains a small amount of fat and vertebral veins. Beneath the dura mater is a thin and delicate membrane called the arachnoid mater. Beneath the arachnoid mater and in contact with the spinal cord is the pia mater. The pia mater is a highly vascularized membrane providing blood to the spinal cord. The space between the arachnoid mater and pia mater is the subarachnoid space. It is filled with cerebrospinal fluid (CSF), which surrounds the entire brain and spinal cord. The subarachnoid space is continuous around the CNS (brain and spinal cord), hence substances released into the space at one location quickly diffuses to other locations.

CSF is secreted from the choroids plexus, a vascular part in the ventricles of the brain. CSF bathes and circulates among these tissues and acts as a shock absorber to protect against injury. CSF is low in cells and proteins, but generally similar to plasma in its ionic composition. Water and soluble substances are freely exchangeable between the CSF and the interstitial fluid of the nervous tissue. The epithelium of the choroid plexus represents a barrier between the blood and the CSF, known as the blood-CSF barrier. Many substances that can leave the capillaries of the choroids plexus cannot enter the CSF. This is important because neurons are extremely sensitive to changes in the composition of their environment. The rate of formation of new cerebrospinal fluid (an average of about 350 µl/minute in man) is relatively constant and little affected by blood pressure or intraventricular pressure. This means that the total volume of CSF is renewed more than three times per day. Most of this fluid is returned to the venous system through small arachnoid villi that are found in the ducal sleeves accompanying spinal nerve roots.

The blood brain barrier (BBB) exists in the brain and spinal cord, separating them from the circulating blood, and serves two main purposes: (a) to control the composition of the brain interstitial fluid and CSF within extremely fine limits, to maintain neural function, and (b) to protect the brain from toxins. The non-fenestrated endothelial cells that form the walls of blood capillaries in the brain and spinal cord, as well as their minimal pinocytotic activity, both contribute to the properties of the BBB. The significance of the BBB to drug delivery is that as a rule, only lipid-soluble small molecule drugs administered systemically can cross the BBB into the brain or spinal cord parenchyma.

1.3.3. Methods of protein drug delivery to the spinal cord

Methods of administration effective for low molecular weight drugs, i.e. oral and systemic administration cannot be used for protein drugs. Oral administration is not suitable because proteins are susceptible to degradation in the gastrointestinal tract. Parenteral systemic administration (intravenous, subcutaneous and intramuscular routes) is not expected to result in significant concentrations of protein drugs in the spinal cord tissue due to the existence of the blood-brain and blood-CSF barriers. These limitations necessitate the development of alternative methods for delivery of protein drugs to the spinal cord. These methods bypass the blood-brain and blood-CSF barriers and include: (a) direct delivery of the proteins either to the CSF or intraparenchymally, and (b) implantation of cells genetically engineered to secrete the therapeutic protein [28]. The former is of particular relevance to this work and will be discussed in further detail in sections 1.3.3.1 and 1.3.3.2.

1.3.3.1. Intrathecal infusion

Delivery of protein drugs to injured neurons via the CSF can be achieved by intrathecal injection/infusion into the CSF in the subarachnoid space either at the level of medulla/cervical spinal cord (intracisternal) or lumbosacral spinal cord (intralumbar). Proteins administered into the subarachnoid space CSF enter the spinal cord parenchyma (tissue) by diffusing through the pia mater and will be limited by the circulation and clearance of CSF, which occurs rapidly compared with the time required for appreciable diffusion into the surrounding tissue. Intrathecal infusion pumps are currently used

clinically to deliver analgesics for chronic pain and antispasticity drugs for severe spasticity [29]. Continuous intrathecal delivery of potential therapeutic molecules has been widely used in animal spinal cord injury models to characterize the response of injured neurons to the molecules [30, 31]. Although intrathecal delivery allows long term administration of agents, easy termination of treatment and highly controllable dosages, there are some serious limitations which pose considerable restrictions for practical clinical use. Catheterization of the subarachnoid space is an invasive technique, which may require a hemilaminectomy for exposure of the vertebral interspace. Also, implantation of the catheter can cause adverse reactions, such as chronic inflammation and dural fibrosis, or result in spinal compression or infection, as has been shown in rodents and dogs [32]. A second intervention is also required to remove the catheter and pump. The distribution of the infusate in the subarachnoid space is not localized, and the agents may be redistributed to the systemic and cranial circulation without reaching the intended target. This is shown by the discovery that continuous intrathecal infusion of ciliary neurotrophic factor in humans led to side effects including development of pain syndromes [33].

Although encouraging results have been attained in SCI animal models, intrathecal drug delivery techniques still have significant limitations. An optimal drug delivery system should provide delivery of the desired agent at the site of injury to prevent systemic side effects. Moreover, the delivery system should not affect the spinal canal environment.

1.3.3.2. Intraparenchymal delivery

In animal models for spinal cord injury, localized delivery of protein drugs have been achieved by [28]: (a) intraparenchymal infusion using cannulas connected to osmotic minipumps, and (b) entrapment of the drug within slow release materials such as gelfoam, fibrin glue, polymerized collagen, and biodegradable polymer microspheres or nanospheres and subsequent implantation at the site of injury. Such localized delivery methods minimize the risk of inducing side effects on neural systems that are not the target of the treatment.

Efficacy of intraparenchymal delivery has been demonstrated in rat models, where infusion of nerve growth factor (NGF) into the spinal cord parenchyma was found to induce ingrowth of sensory fibers [28]. Intraparenchymal delivery using an osmotic minipump offers the same advantages as intrathecal delivery. However limitations include the requirement of a chronically implanted cannula, which means multiple surgical interventions are necessary. Insertion of a cannula can also cause tissue damage and prolonged use of cannulas can result in tissue reaction around the cannula, leading to clogging of the cannula, which then prevents continuous protein delivery.

In the second method where the drug is entrapped in slow release polymers, the drug gradually diffuses out once the polymer is implanted, or is released as the polymer naturally degrades, hence providing supply of the drug for a prolonged period of time. Gelfoam, collagen and fibrin matrices have been shown to be beneficial in spinal cord regeneration, as they can serve as physical bridges across the lesion site for neurite

extension [34]. However, such matrices have the disadvantage that the rate of delivery cannot be controlled and the administered drug may be rapidly depleted due to rapid diffusion out of the matrix. An alternative method is to encapsulate the drug in biodegradable polymeric microspheres, which can then be administered by injection directly into the spinal cord parenchyma. By carefully choosing the polymer and its configuration it is possible to predetermine the rate of release for the particular drug.

1.3.4. Delivery of C3 transferase to the spinal cord

For successful treatment of spinal cord injury with C3, two major requirements must be met. First, as C3 displays non-specific activity in non-neural tissues, it must be delivered directly into the injured site of the spinal cord. Investigations of the temporal changes in expression of inhibitory molecules at the lesion site indicates prolonged persistence of these proteins in degenerating fibre tracts, which may contribute to the maintenance of an environment that is hostile to axonal regeneration. In mature mammals, CSPGs are secreted rapidly within 24 hours after injury and can persist for many months [35]. Myelin associated proteins including Nogo were detected in post-mortem spinal cords of patients even three years after injury [36]. Therefore, the second requirement for C3 treatment is that administration of C3 should be sustained for an extended period of time.

Two methods of continuous delivery which have been tested in mouse models of spinal cord injury are continuous intrathecal infusion of C3 solutions using an osmotic minipump [14] and release from collagen gels and fibrin soaked with C3 solutions [16].

They both have major limitations which can affect clinical efficacy of C3 treatment. The risks of intrathecal delivery in clinical applications are high due to the possible non-specific effect on neuronal systems that are not the target of the treatment. In the gel delivery method, C3 was first added to a solution of either fibrinogen or collagen and applied to the lesion site. Polymerization of the solution occurred after application to the lesion, forming a gel entrapping C3. This formed a reservoir of C3 immediately available to the injured neurons. Although the use of collagen and fibrin matrices in SCI is beneficial as they support tissue repair, there are significant limitations preventing their practical use. Studies using simple admixtures of other protein drugs with fibrin have demonstrated a large uncontrolled burst release of 70-100% of the drug within the first 24 hours [37, 38]. Sustained release of therapeutic molecules from collagen matrices is also beset with difficulties as fibrillar collagen gels have an effective pore size of several tens of nanometers, too large to control release by hindered diffusion [39]. As with fibrin matrices, collagen matrices have poor loading capacity for protein molecules. Hence without further modifications, for example by creating affinity sites on the gel to bind C3, or by chemically coupling C3 molecules to the gel matrix, the matrices would be rapidly depleted of the C3 protein, and this clearly limits their use for long term regeneration therapy.

To harness the promising therapeutic potential of C3 in spinal cord injuries, microencapsulation of C3 in poly(D,L-lactide-co-glycolide) (PLGA) microspheres is proposed as an alternative approach for sustained release. PLGA is biocompatible to spinal cord tissue and degrades to toxicologically acceptable products that are eventually

eliminated from the body [40]. C3 is gradually released as the microspheres degrade and erode. The rate at which release occurs can be controlled by the properties of the PLGA used. Microencapsulation of C3 will be advantageous as neurons will not be exposed to the entire dose of the protein at one time, but instead, will receive a constant and consistent daily dose over a prolonged period of time.

1.4. Microencapsulation of protein drugs

Entrapment of protein drugs within microparticulate drug delivery systems, using various types of biodegradable polymers, has been studied during the past two decades. Such controlled-release devices can be engineered to provide precisely controlled, prolonged protein drug delivery at a localized site. An additional advantage of using biodegradable polymers is that such additional surgery is not required to remove the devices. At the time of writing, there has been no commercial microencapsulated protein drug meant for treatment of spinal cord injury. However, clinical efficacy of microencapsulated drugs have been demonstrated in other applications and these include recombinant human growth hormone (Nutropin Depot®, Genentech-Alkermes) and leuprolide acetate (Lupron Depot®, Takeda-Abbott) [41, 42].

One of the most common methods of preparing microspheres involves emulsification and subsequent organic solvent evaporation [43]. Two techniques of emulsification are normally used: the water-in-oil-in-water (w/o/w) or the solid-in-oil-in-water (s/o/w) emulsion systems. The steps in w/o/w technique are illustrated in Fig 2.

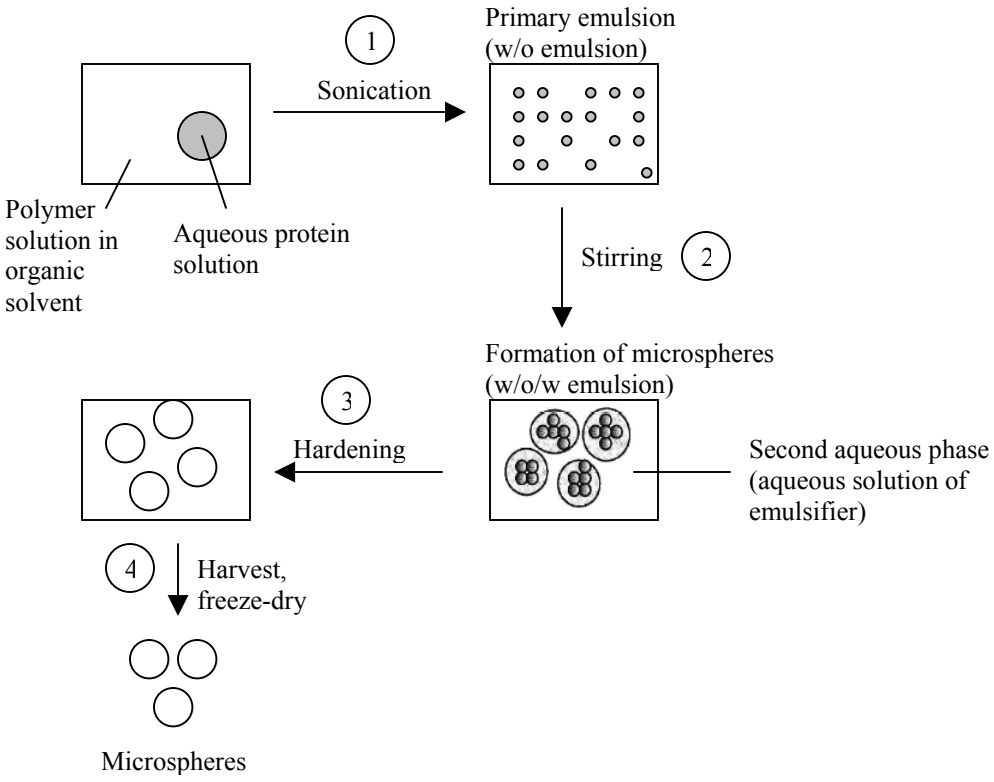

Fig. 2: Encapsulation of a protein into microspheres following a typical w/o/w emulsification technique. (1) Primary emulsification: aqueous solution of protein is emulsified into a polymer solution, (2) Re-emulsification: primary emulsion (w/o) is further emulsified into a second aqueous phase containing a stabilizer PVA to form w/o/w double emulsion, (3) Solidification: the organic solvent is extracted in the continuous aqueous phase resulting in precipitation of polymeric microparticles, (4) Separation and purification: microspheres are collected by centrifugation or filtration and subsequently freeze-dried.

Most protein microencapsulation studies have used poly(lactic acid) (PLA) or PLGA. PLGA and PLA are the most investigated and advanced polymers with regard to available toxicological and clinical data [40]. These polymers are non-toxic, biocompatible and biodegradable and approved by the Food and Drug Administration for human use. PLGAs (Fig. 3) undergo *in vivo* and *in vitro* degradation in an aqueous environment by means of hydrolytic cleavage of their backbone ester linkages. The degradation products are lactic and glycolic acid which are easily eliminated from the body. Hydrolysis of ester bonds can be catalysed by free carboxyl end groups within the same molecule (intramolecular catalysis) or by other acidic moieties such as lactic and glycolic acids, products of PLGA degradation that accumulate within the hydrated microsphere (intermolecular catalysis) [40].

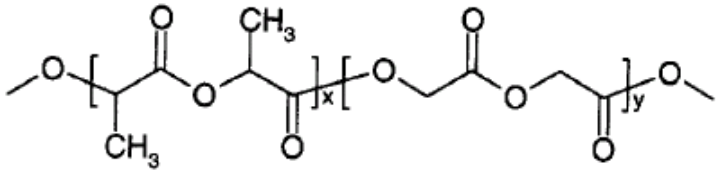

Fig. 3: Chemical structure of PLGA (x = lactic acid monomer, y = glycolic acid monomer).

Work on encapsulation of low molecular weight drugs and peptides in microspheres have been well established. However, delivery of large proteins using microspheres is much more challenging because of several reasons. The larger size and complex, well defined tertiary/quaternary structure has bearing on release behavior and stability during the encapsulation process and release from microspheres. Two critical issues must be addressed in order to ensure continuous delivery of biologically active protein from

PLGA microspheres for an extended period of time: the control of the protein release kinetic profile and the retention of biological activity after release. It is important to obtain continuous cumulative release of over 90% of encapsulated protein during the treatment period with a concomitant retention of sufficient biological activity [44].

1.4.1. Protein release characteristics

For low molecular weight drugs, release from microspheres occurs by classical partition-dependent diffusion [45]. The large size of proteins and their insolubility in polymers means that such diffusional transport through the polymer phase is minimal. Hence release of protein from PLGA microspheres is largely dependent on diffusion through existing water-filled pores or on polymer degradation and subsequent polymer erosion.

The dependence of protein release on polymer degradation can be understood if the degradation and erosion process in an aqueous environment is first considered. Four stages in the *in vitro* degradation of PLGA can be distinguished and these are indicative of the bulk erosion process [46] (Fig. 4):

(a) an initial lag period during which hydration of the polymer occurs

(b) random ester bond cleavage throughout the polymer matrix, resulting in a decrease in molecular weight (but no microsphere erosion yet)

(c) continued bond cleavage to a critical molecular weight resulting in onset of polymer mass loss (i.e. onset of microsphere erosion), caused by solubilization of the low molecular weight polymer fractions

(d) complete solubilization (i.e. complete microsphere erosion)

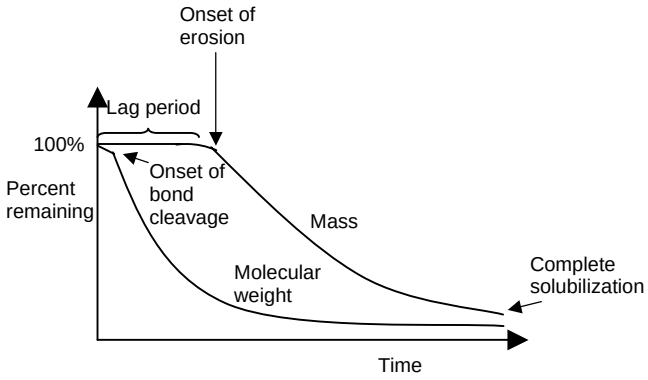

Fig. 4: *In vitro* degradation of PLGA immersed in aqueous solution.

Generally, depending on the type of PLGA used, release of encapsulated proteins from microspheres immersed in an aqueous environment occurs in three phases that follow the stages of degradation of the polymer [47]. Within 24-48 hours after hydration, protein located at or near the surface of microspheres dissolves and diffuses out into the medium. This first phase is commonly known as the initial burst. This phase is followed by a diffusional release phase during the period before erosion of the polymer matrix begins. The diffusional release occurs through water-filled networks of pores and channels, hence is dependent on the rate of water uptake into the microspheres and the level of existing porosity within the matrix. In the third phase, erosion of the polymer occurs resulting in pore formation and fragmentation of the microspheres thus enhancing drug release. This phase is also sometimes known as the 'second burst'. The second burst has been shown to coincide with the onset of mass loss of the polymer matrix. The penetration of water is a critical factor in the chain of events leading to the depletion of drug from a degradable depot because both drug diffusion and polymer matrix erosion are driven by water ingress.

The degradation rate of PLGA microspheres is dependent upon such factors as the polymer physicochemical properties (e.g., molecular weight, lactide/glycolide ratio, endgroup chemistry, crystallinity), microsphere properties (e.g., size, surface morphology, porosity) and environmental factors (e.g., aqueous medium, pH, temperature), all of which affect accessibility of the ester linkage to water [44, 48, 49]. These properties of PLGA microspheres determine the degree of hydrophilicity of the matrix, and therefore rate of water uptake into the matrix, degradation kinetics and rate of protein release. PLGA polymers with physicochemical properties such as lower molecular weight, lower lactide/glycolide ratio and free carboxylic endgroups have been shown to exhibit a higher degree of hydrophilicity and therefore, hydrolytic cleavage of polymer chains begins earlier and at a higher rate [48]. Microsphere properties such as surface morphology, internal porosity and size can be controlled by the production parameters in the double emulsion process. For example, the final internal porosity is controlled by both the volume ratio of internal aqueous solution to the organic phase and the method of emulsification of the primary emulsion [50].

Depending on the degradation kinetics of the polymer, two main types of release profiles have been reported for protein drugs. A biphasic or parabolic profile [51] arises if protein diffusion is significant during the diffusional phase of release so that a continuous release is seen up to the point when polymer erosion begins. A triphasic or S-shaped profile [52, 53, 54] is obtained if protein diffusion is minimal during diffusional phase, giving rise to a lag period. At the onset of matrix mass loss, the release of protein increases dramatically, giving rise to a second burst.

1.4.2. Methods to modulate release characteristics

As was discussed in the previous section, the rate of water uptake by the microsphere matrix determines the rate of degradation of the polymer, and this in turn affects the rate of release of the entrapped protein drug. Customization of release characteristics for a particular application is important to ensure clinical efficacy. In this respect, the knowledge that the rate and extent of water ingress by the microsphere matrix is dependent on microsphere microstructure and polymer physicochemical properties has been used to develop methods for controlling drug release characteristics. In some cases where the use of entirely new polymers is not of interest, approaches which exploit the properties of existing polymers can be used.

One of the approaches is to manipulate the porosity of microspheres, such that the release of protein is primarily via diffusion through interconnected pores or channels in the microspheres. In this way, protein diffusion is significant after the initial burst, hence eliminating the lag period. To achieve this, studies which involve the incorporation of poly(ethylene glycol) (PEG) into a poly(D,L-lactide) matrix have been carried out [55]. The addition of the hydrophilic PEG led to increased water uptake and its dissolution in the release medium creates more water channels, thereby allowing diffusion of the acidic degradation products out of the polymer. This gives rise to a release profile that is characteristic of diffusion through water-filled pores in the microsphere. A major disadvantage of this method is that the water soluble nature of PEG will also lead to lower entrapment levels of the protein. In another recent study [56], built-in nano-porous and interconnected channels within the microspheres were obtained by judiciously

selecting a low molecular weight poly(L-lactide) as the matrix material. Entrapped proteins were released completely, in a diffusion-controlled manner. However, a drawback of this method is that the slowly degrading PLA microspheres may elicit undesirable foreign body reactions when administered into the body.

The second approach to modulating release profile involves fine-tuning the degradation rates of the polymer, either by copolymerizing or physical blending of different polymers. In this way, polymer erosion begins early in the incubation period to achieve drug release even during the initial period, when release is normally governed by dissolution and diffusion of solubilised drug from the polymer matrix. Blending of polymers with faster degradation rates have been shown to increase the release rates in the period after the initial burst [57, 58, 59]. In one study [57], bovine serum albumin (BSA) loaded microspheres prepared with 75:25 PLGA alone showed very little degradation in the first 24 days, resulting in minimal release of BSA. When amorphous D,L-PLA with a low molecular weight of 2000 Da was blended with the 75:25 PLGA in a suitable proportion, the degradation rate increased and zero-order release kinetics were observed. It was found that the incorporation of D,L-PLA into the microspheres led directly to an increased rate of water uptake, thereby increasing its degradation and erosion rate, creating pores through which BSA can diffuse out of the microspheres.

1.4.3. Protein stability

Apart from release characteristics, a very important criterion for microspheres is the capacity to deliver the protein drug in a biologically active form. Protein stability can be compromised during the various stages of microsphere processing, storage and application. Protein instability can be of chemical or physical nature. Physical instability develops through conformational changes leading to denaturation, surface adsorption, aggregation or precipitation of the protein. Chemical instability can occur as a result of chemical reactions such as oxidation and hydrolysis. The causes of protein instability as well as the methods used to minimize instability have been extensively reviewed [60, 61].

In this section, two major causes of instability and the approaches used to maintain protein integrity are briefly highlighted. First, the sonication step in the commonly used water-in-oil-in-water emulsification technique is a major cause of degradation [62]. The sonication step is necessary for generating homogenous dispersions but can denature proteins through large pressure and temperature gradients and high shear forces [62]. In addition, sonication exposes the protein to the denaturing action of organic solvent across a large interfacial area. To prevent emulsification-induced denaturation, excipients have been added to the inner aqueous phase. Some excipients such as bovine serum albumin [63], PEG 3350 [64], PEG 400 [65], gelatin [66] work by accumulation at the water/organic solvent interface, thereby shielding the interface from the protein drug. During release, a major cause of protein degradation is the acidification of the environment as the polymer degrades [67]. This can cause aggregation and denaturation of the protein, leading to incomplete release, or release of inactive protein. To inhibit

acid-induced protein degradation during release, poorly water soluble basic inorganic salts such as magnesium hydroxide [68] have been incorporated into the microspheres.

1.5. Motivation and Objectives

Methods which have been used for the delivery of C3 transferase to the spinal cord injury site have so far been inadequate to ensure successful therapy clinically. As such, there is a need to develop a delivery system which allows the rate of release to be controlled, thereby ensuring a continuous supply of active C3 in therapeutic amounts during the entire treatment period. The use of PLGA microspheres as a delivery vehicle for C3 is proposed as an alternative approach for sustained release. The rationale for this choice is that the rate of release of C3 incorporated within PLGA can be tightly coupled to the degradation rate of the matrix, and hence can be controlled by judicious selection of polymers.

The objective of this study was to encapsulate C3 transferase within PLGA microspheres to produce a sustained release formulation that will deliver active C3 in therapeutic amounts in the time period needed for axonal regeneration. As pre-clinical studies of C3 are still in the initial stages, clinically relevant amounts of C3 and the period of release have not yet been established. Previous studies in animal spinal cord injury models indicate that continuous supply of C3 for a period of one month may be necessary for C3 to show its positive therapeutic effects [16]. In addition, due to the high potency of C3, daily supply of nanogram levels of C3 may be sufficient.

In particular, two major issues were addressed in this study. First, the poor cellular uptake of native C3 necessitates the addition of a protein transduction domain to C3 to ensure efficient uptake. In this respect, a domain derived from the Tat protein of the human immunodeficiency virus was used as it has been shown to improve cellular uptake significantly and does not affect C3 activity. By increasing the efficiency of C3 entry into cells, lower concentrations of C3 can be used, hence minimizing toxicity issues. The second issue is the control of the protein release characteristics. In this study, the efficacy of blending two PLGA polymers with different physicochemical properties as a method of modulating release characteristics was investigated.

In order to evaluate the feasibility of using C3 microspheres to promote the long term regeneration of injured neurons, an *in vitro* study assessing the microsphere degradation characteristics as well as C3 release characteristics and activity of released C3 was carried out.

CHAPTER TWO

MATERIALS AND METHODS

2.1. Materials

2.1.1. Solutions and reagents for purification of C3 transferase

RIPA lysis buffer: 50 mM Tris.Cl, 150 mM NaCl, 1% NP40, 1 mM $Na_4P_2O_7$, 1 mM NaF, 1 mM EDTA, 2 mM Na_3VO_4, 1x protease inhibitor cocktail (Roche).

10× thrombin cleavage buffer: 500 mM Tris.Cl pH 8.0, 1.5 M NaCl, 25 mM $CaCl_2$, 20 mM $MgCl_2$, 10 mM dithiothreitol.

Sample buffer for SDS-PAGE: 125 mM Tris.Cl pH6.8, 25% glycerol, 2% SDS, 5% β-mercaptoethanol, bromophenol blue.

Coomassie Blue staining solution: 2 tablets of R250 Coomassie blue (R250, Merck), 50 ml methanol, 12.5 ml acetic acid, 75 ml ddH_2O.

Coomassie Blue destaining solution: 20 ml acetic acid, 60 ml methanol, 120 ml ddH_2O.

Gel drying solution: 8 ml glycerol, 90 ml methanol, 102 ml ddH_2O.

2.1.2. Materials for microsphere preparation

Two types of PLGA 50:50 polymers, with different polymer end groups, were used to investigate the effects of blends of different ratios of the two polymers on the release profile. The polymer endgroup is determined by the choice of initiator used in the polymerisation reaction. Uncapped PLGA contains free carboxyl end groups at the polymer terminus, which cause increased hydrophilicity, faster and larger extent of water uptake and hence faster degradation in aqueous environments [69]. Capped PLGA contains hydrophobic lauryl ester groups at the polymer terminus which give a hydrophobic property to the polymer. The polymers were purchased from Alkermes and their weight-average molecular weights as determined by gel permeation chromatography were 35000 Da for the capped polymer and 12500 Da for the uncapped polymer. Polyethylene glycol (PEG, M_w 3350, Sigma) was included in the C3-Tat solution at a C3: PEG mass ratio of 1:4. PEG has been shown to be effective in stabilizing basic proteins during the w/o/w double emulsion process [65].

2.2. Preparation of cDNA encoding recombinant C3 transferase

cDNA encoding C3 transferase in the plasmid pGEX2T was kindly provided by Dr. Lamarche V.N. (McGill University, Department of Anatomy and Cell Biology, Montreal, Canada). The DNA construct was modified by recombinant DNA techniques to add the Tat peptide and hemaagglutinin (HA) peptide to the N-terminal of C3 transferase. The amino acid sequences for Tat and HA are YGRKKRQRRR and YPYDVPDYA respectively. The full amino acid sequence of C3 transferase can be found under the

NCBI accession number CAA35828.

To achieve this, KpnI and EcoRI restriction sites were first added to the 5'and 3'ends of C3 transferase by PCR, respectively, using the forward primer C3F2 [5'-aaggtaccgcttattccattaatcaa-3'] and reverse primer C3R2 [5'-aagaattctctttaggattgatagctgt-3'] and pGEX2T-C3 as the DNA template. The PCR product was first subcloned into pCAP plasmid vector using EcoRV restriction site, and then released with KpnI and EcoRI restriction enzymes. The resulting DNA fragment was then subcloned into pHM6 plasmid vector (which contains the HA tag) using KpnI and EcoRI sites, creating pHM6-C3. The sequence of this plasmid was first verified by DNA sequencing to be correct, before proceeding with the next step. In the next step, the primers Tat-S [5'-gcatatgtacggtcgtaaaaaacgtcgtcagcgtcgtcgtggt-3'] and Tat-AS [5'-ctagaccacgacgacgctgacgacgttttttacgaccgtacatatgc-3'] were self-annealed and then subcloned into pGEXKG plasmid vector via SmaI and XbaI sites, creating pGEXKG-Tat. This plasmid was sequenced to verify that Tat has been incorporated correctly.
Using another set of primers XbaHAF1 [5'-aatctagaatacccatacgacgtccca-3'] and HM6R1 [5'-ggcacagtcgaggctgatca-3'], and pHM6-C3 as the template, the HA-C3-His6-Stop fragment was PCR amplified to incorporate an XbaI restriction site at the 5' end. The PCR product was digested with XbaI and SacI restriction enzymes and the resulting fragment subcloned into pGEXKG-Tat via XbaI and SacI restriction sites. This results in the final expression construct, pGEXKG-Tat-HA-C3 which upon expression and purification will yield the desired recombinant C3 transferase, with Tat peptide and HA tag at the amino terminal of C3. DNA sequencing confirmed the correct sequence of the

pGEXKG-Tat-HA-C3 plasmid.

As a control in subsequent experiments, an expression construct for C3-HA without the Tat peptide attached was also prepared. This protein is designated as unmodified C3. For this, the XbaI and SacI digested HA-C3-His6-Stop fragment prepared earlier was subcloned into a pGEXKG plasmid via Xba1 and Sac1 restriction sites.

2.3. Purification of recombinant C3 transferase

The pGEXKG plasmid is designed for inducible expression of genes as fusions with glutathione S-transferase protein (GST) in *E. coli* bacteria. The pGEXKG-Tat-HA-C3 construct was transformed into protease deficient BL21 *E. coli* to purify the desired C3-Tat protein. The pGEXKG-HA-C3 construct was also transformed into BL21 to purify unmodified C3. A single colony was picked from a fresh transformation plate containing 50 μg/ml ampicillin and inoculated into 12 ml Luria broth (LB) containing 50 μg/ml ampicillin. The cells were grown at 37 °C for 16 hours. The overnight culture was diluted 1:10 in 100 ml fresh LB containing 50 μg/ml ampicilin, and grown for an additional 1 hour at 37 °C. Expression of the fusion protein was induced by addition of isopropyl β-D-thiogalactoside (IPTG) to a final concentration of 0.5 mM, and then the culture was incubated for another 3 hours at 37 °C. The cells were pelleted by centrifugation at 8000 rpm for 5 minutes at 4 °C. The cell pellet was resuspended in 10 ml ice-cold 1x PBS and then lysed on ice with a probe sonicator, using 10 × 10 second bursts and 10 second rest intervals. Insoluble cell materials were removed by centrifuging the lysate at 13000 rpm

for 10 minutes at 4 °C.

The soluble GST fusion proteins were purified from the supernatant by affinity chromatography on glutathione sepharose 4B (Amersham Biosciences). The process is shown in Fig. 5. A 1 ml bed volume of the beads in a 15 ml Falcon tube was prepared according to the manufacturer's instructions. The cleared cell lysate was added to the beads and incubated for 1 hour at 4 °C with gentle agitation on an orbital shaker. The suspension was centrifuged at 2000 rpm, 4°C for 5 minutes. The supernatant was removed and the beads were washed 3 times with 10 ml 1× PBS. The pGEXKG plasmid is designed with a thrombin cleavage site upstream of the multiple cloning site. Incubation of the GST fusion protein on beads with thrombin results in release of the protein of interest from the GST tag. 10 units of thrombin (Amersham Biosciences) in 1× thrombin cleavage buffer at a final volume of 1 ml were added to the beads, and the beads were incubated for 9 hours at 4 °C with gentle agitation. The suspension was centrifuged at 2000 rpm for 5 minutes and the supernatant transferred to a fresh tube. To remove thrombin from the purified C3-Tat, 100 µl of p-aminobenzamidine agarose beads (Sigma) was added to the supernatant, and incubated for 30 minutes at 4 °C with gentle shaking. Finally, the p-aminobenzamidine agarose beads with the bound thrombin are pelleted by centrifugation. Any remaining cleaved C3 associated with the sepharose beads was recovered with 500 µl 1× thrombin cleavage buffer.

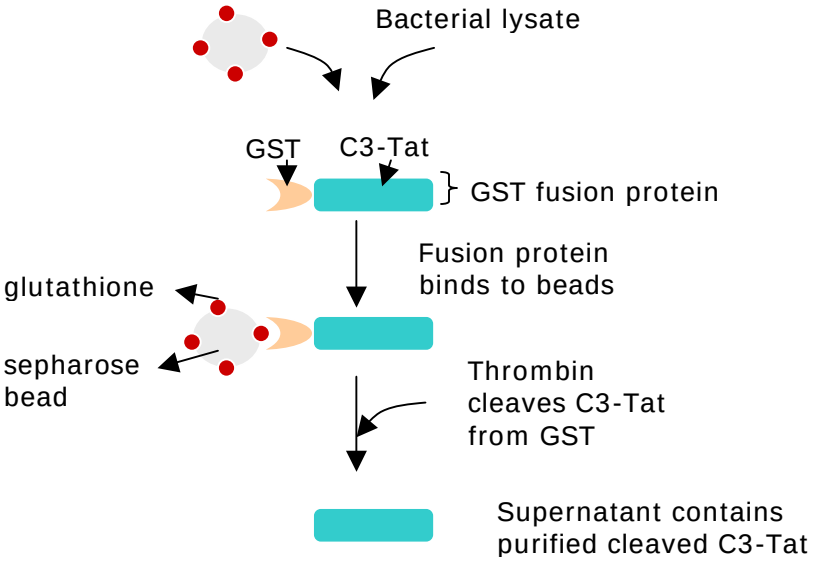

Fig. 5: Schematic representation of the purification process of recombinant C3-Tat.

2.4. Sodium dodecyl sulfate-polyacrylamide gel electrophoresis (SDS-PAGE)

The purity of cleaved C3 from each preparation was determined by Coomassie staining of SDS-PAGE gels and confirmed by Western blot. Samples were mixed with sample buffer and boiled at 95°C before loading onto a 10% SDS-PAGE gel.

2.4.1. Coomassie blue staining

Proteins were visualized by incubating the polyacrylamide gel in Coomassie staining solution overnight at room temperature with gentle shaking. Destaining was performed with destaining solution until the background staining was eliminated and the protein bands were clearly visible. The gel was dried by incubating in a gel drying solution for 2 hours, and then mounted using the DryEase Mini-Gel Drying System (Invitrogen).

2.4.2. Western blot

Following electrophoresis, protein samples on the gel were transferred onto nitrocellulose membrane (Shleicher & Schuell Bioscience) for 1 ½ hours at 100 V using a wet transfer apparatus (Biorad). The membranes was incubated in blocking buffer (2% skimmed milk powder in 1× PBS) for 1 hour, followed by an appropriate dilution of anti-HA (Santa Cruz) primary antibody. The membrane was washed 3 times with 1× PBS, for 10 minutes each. This was followed by incubation for 1 hour with an appropriate dilution of the anti-rabbit secondary antibody conjugated to horseradish peroxidase (Pierce). The membrane was washed 3 times as previously described. All incubation steps were performed at room temperature with gentle agitation on an orbital shaker. The membranes were developed using Supersignal West Pico (Pierce) substrate.

2.5. Protein quantification

Prior to microencapsulation, the purified C3-Tat solutions from different preparations were pooled together and the protein concentration determined using microBCA assay (Pierce). Purified C3-Tat samples were diluted 15-fold in ddH_2O for the assay. Bovine serum albumin (BSA) (Sigma A7906) was used as standards and stock BSA solutions in 1×PBS were used to perform serial dilutions from 200 to 0.5 µg/ml. The linear range for this assay is between 2 – 40 µg/ml. Assay procedures were as described in the manufacturer's manual. Absorbance was measured at 562 nm using a plate reader (Tecan Spectra Rainbow Thermo). The standard curve was used to determine the relative protein concentration of each sample.

2.6. Determination of C3-Tat cellular uptake efficiency

The efficiency of uptake of the purified C3-Tat into cells was determined by immunostaining experiments. NIH3T3 fibroblast cells were grown in Dulbecco's modified Eagle's medium (DMEM) with 10% fetal bovine serum (FBS) and 1% penicillin-streptomycin (P/S) in a T75 culture flask. 2.7×10^4 cells were plated on 12 mm circular glass coverslips in a 24-well culture plate and left at 37 °C for 4 hours to allow them to settle. After the cells have adhered to the coverslips, the medium was removed and replaced with fresh DMEM, with 10% FBS and 1% P/S, together with 10 μg/ml of purified C3-Tat or unmodified C3. The cells were incubated at 37°C for 24 hours. The medium was removed and the cells were washed three times with 1×PBS. The cells were then fixed in 4% paraformaldehyde for 10 minutes, and then washed three times with 1×PBS. The cells were permeabilised with 0.2% TritonX-100 for 5 minutes, and then washed three times with 1×PBS. Next, the cells were blocked with 3% BSA in 1×PBS for 1 hour. The cells were then probed with anti-HA antibody (Santa Cruz) diluted to 1:100 in 3% BSA. After 1 hour, the antibody solution was discarded and the cells were washed three times with 0.1%BSA in 1×PBS. Next the cells were probed with secondary antibody (α-rabbit Alexa Fluor 488, Molecular Probes) at 1:1000 dilution in 3% BSA. After 1 hour incubation in darkness, the cells were washed with 0.1% BSA. An antifading solution (FluorSave, Calbiochem) was used to mount the coverslips on glass slides. The cells were viewed with a fluorescence microscope (Leica).

2.7. Determination of *in vivo* biochemical activity of C3-Tat

The ADP-ribosylation of RhoA by C3-Tat can be detected as an upshift in molecular weight of intracellular RhoA on a Western blot. The intracellular activity of purified C3-Tat was determined by western blot analysis of cells treated with the enzyme. Briefly, NIH3T3 cells were plated in a 6-well culture plate at a density of 3.5×10^5 cells/well. The cells were incubated at 37°C for 4 hours to allow them to settle. The medium was removed and replaced with complete medium containing either 5 µg/ml or 10 µg/ml C3-Tat. Complete medium alone was added to one well to serve as treatment control. The cells were incubated at 37°C for 24 hours. To harvest the cells, they were washed 3 times in 1×PBS, and scraped off the plate with a rubber policeman. The cells were lysed in RIPA lysis buffer and then clarified by centrifugation. The amount of protein in the cleared lysate was determined using BCA assay (Pierce) and 60 µg of protein was separated on a 12% SDS-PAGE gel. The proteins were transferred to nitrocellulose membrane as previously described in section 2.4.2. The membrane was probed with anti-RhoA antibody (Santa Cruz) at a 1:200 dilution, followed by an anti-mouse-HRP antibody (Pierce) at a 1:5000 dilution. The membrane was detected with Supersignal West Femto (Pierce) substrate.

2.8. Preparation of microspheres

Microspheres containing C3-Tat were prepared using a water-in-oil-in-water (W/O/W) emulsion method adapted from Pean *et al* [65]. First, a 180 μl aqueous solution of purified C3-Tat (100 μg/ml) and PEG (C3:PEG mass ratio of 1:4) was emulsified in 2.34 ml dichloromethane containing 117 mg PLGA (single or a combination of polymers). Emulsification was performed in an ice bath, using a probe-type sonicator (XL2000, Misonix) at 3W output for 10 seconds. This water-in-oil emulsion was then added into an external aqueous solution of PVA (5% w/v, 35 ml) and stirred at 500 rpm for 1 minute on a magnetic stirrer. The resulting water-in-oil-in-water emulsion was added to deionised water (300 ml) and magnetically stirred at 500 rpm for a further 30 minutes to extract and evaporate the organic solvent. The formed microspheres were washed 3 times with deionised water and freeze-dried overnight to obtain a fine white powder. The freeze-dried microspheres were stored at 4°C until further analysis. Blank microspheres were prepared in the same way, but with deionised water as the internal aqueous phase.

2.8.1. Polymer blending

To evaluate the effect of polymer blends on the C3-Tat release profile, C3-Tat microspheres were prepared at 100/0, 70/30, 50/50, 30/70 and 0/100 ratios of capped/uncapped PLGA. The samples were named 100/0, 70/30, 50/50, 30/70 and 0/100 respectively. Blank microspheres were also prepared using the same ratios.

2.9. Determination of morphology and internal microstructure of microspheres

A scanning electron microscope (SEM) (Model JSM-5600LV, JEOL) was used to examine the surface morphology and internal microstructure of blank microspheres before and after *in vitro* degradation studies. Cross-sectioned microspheres were prepared by slicing the freeze-dried microspheres with a razor blade. Microspheres and their section samples were placed on metal stubs using double sided carbon tape and sputter-coated with platinum.

2.10. Determination of microsphere size

Diameters of 100 microspheres were determined from representative SEM images using the SmileView software and values were expressed as mean ± standard deviation.

2.11. Determination of microsphere encapsulation efficiency

The levels of C3-Tat encapsulated in microspheres were determined using a method similar to that reported by Yan *et al* [70]. A known amount of microspheres (~10 mg) was added to 0.9 N sodium hydroxide (150 µl) and shaken on an orbital shaker at room temperature for 4 hours. When the microspheres were solubilized completely, the resulting clear solution was neutralized to pH 7.0 by a few drops of 0.9 M hydrochloric acid. The amount of C3-Tat in the solution was determined by the microBCA assay as described in section 2.5. Measurements were performed in triplicate and the results are presented as mean ± standard deviation. Encapsulation efficiency was calculated using

equation 1, by comparing the amount of protein in the solubilized microspheres as detected by the microBCA assay (W_{actual}) with the amount of protein that should theoretically be contained in the same amount of microspheres ($W_{theoretical}$).

$$\text{Encapsulation efficiency (\%)} = W_{actual} / W_{theoretical} \times 100 \quad (1)$$

The microBCA assay is based on the reduction of Cu^{2+} ions to Cu^{1+} ions by protein in an alkaline medium and the colorimetric detection of the Cu^{1+} ion using a reagent containing bicinchoninic acid (BCA) [71]. While protein is unlikely to be decomposed in 0.9N sodium hydroxide, it may be cleaved into smaller peptides. Given the fact that colour formation with BCA is strongly influenced by the presence of any of the four amino acid residues (cysteine, cystine, tyrosine, tryptophan) in protein as well as by the number of peptide bonds, the presence of only a single amino acid residue in the sample still results in the formation of a coloured BCA-Cu^{1+} chelate.

2.12. *In vitro* release studies

The release profile of C3-Tat from microspheres was determined by incubating 10 mg microspheres in 250 µl of a HEPES [4-(2-hydroxyethyl)-1-piperazineethanesulfonic acid] buffer (100 mM HEPES, pH 7.4, 10 mM NaCl) at 37°C with shaking. The studies were performed in triplicate. At predetermined time intervals, the microsphere suspension was centrifuged at 2000 rpm and the supernatant was collected (250 µl) and replaced with fresh buffer (250 µl). The supernatant was stored at -20°C until further analysis.

2.13. Enzyme-linked immunosorbent assay (ELISA)

An ELISA assay was developed to quantify the amount of C3-Tat released from the microspheres. An indirect ELISA format was used, where the antigen (C3-Tat) is bound to the substrate (microplate) and detected with anti-HA primary antibodies and anti-mouse-HRP secondary antibodies. The optimal primary antibody dilution was first determined using a checkerboard titration method with HEPES medium as the coating buffer.

To determine the amount of C3-Tat in the release medium samples, 50 µl of the release samples was added to the microplate wells (Nunc). The standards used were 50 µl purified C3-Tat in HEPES buffer, in a concentration range from 39 to 625 ng/ml. The plate was incubated for 20 hours with shaking at 100 rpm at 4 °C. The solutions were discarded and blocking buffer (1% BSA in 1×PBS) was added and incubated for 1 hour at 100 rpm, at room temperature. The anti-HA antibodies were diluted 1:800 in 1% BSA and 50 µl added to each well. Incubation was for 1 hour, 100 rpm, room temperature. The wells were washed three times with 1×PBS, and then a 1:5000 dilution of anti-mouse-HRP antibodies were added. Incubation was for 1 hour, 100 rpm, room temperature. The wells were washed three times with 1×PBS, and then ABTS substrate (Roche) in acetate buffer was added to each well. After incubation for 30 minutes, the absorbance was measured at 405 nm in a microplate reader. A standard curve from known quantities of fresh C3-Tat was plotted and amount of C3-Tat in release samples were determined from this curve. The value at each time interval was expressed as mean ± standard deviation.

2.14. Determination of change in pH of release medium

The pH of the release medium at different time points was detected using universal pH indicator strips (Merck).

2.15. *In vitro* degradation studies

Ten milligrams of blank microspheres were suspended in 250 µl of HEPES buffer and incubated at 37°C with shaking. For each microsphere formulation, there were three replicate tubes for every time point. At one week intervals, for up to 4 weeks, the tubes were centrifuged and buffer was removed from every tube. Fresh buffer was added to all but one tube. The sample in this tube was freeze-dried for 24 hours. The degraded samples were characterized over time by measurement of molecular weights and residual mass, and observation of microstructure (by SEM).

Polymer mass remaining was calculated according to equation 2 by comparing the mass at a given time point (W_t) to the initial mass (W_o). Measurements were performed in triplicate, and the means were plotted with standard deviation as the error bars.

$$\text{Percentage mass remaining} = (W_t / W_o) \times 100\% \quad (2)$$

Polymer molecular weight was determined by gel permeation chromatography using a column on a HP 1100 LC system (Agilent). 1 mg of microspheres was dissolved in 1 ml tetrahydrofuran (THF), filtered through a 0.45 µm PTFE filter and 20 µl was injected and

eluted with THF at 1 ml/min. Weight-average molecular weights (M_w) were calculated with polystyrene standards (Agilent) with molecular weights 580, 7200, 113000 and 1950000 Da, using the HPChem software.

The degradation rate constant for each microsphere formulation was calculated based on the knowledge that the degradation of polyesters such as PLGA proceeds by random hydrolytic chain scission of ester linkages, which is autocatalysed by the carboxyl-end groups. This process may be described by first order kinetics [72]. The weight average molecular weight (M_w) for each sample, at each time point, was first normalized to the initial weight average molecular weight (M_{wo}). Semilog plots of the normalized weight average molecular weight versus time (in days) were made. The slope was determined by a linear least-squares fit to the data and expressed in units of day^{-1}. The slope represents the first-order degradation rate constant of M_w decay.

2.16. Determination of enzymatic activity of C3-Tat released into release medium

Bioactivity of C3-Tat can be assessed by its catalysis of ADP-ribosylation of RhoA, which results in an increase in molecular weight of RhoA upon Western blot analysis. A modified form of an *in vitro* ADP-ribosylation assay [73] was used in the present study. The cDNA encoding human RhoA in pGEXKG plasmid vector which was kindly provided by Denis Gingras (Universite de Montreal) was transformed into BL21 cells for expression of RhoA as a GST-fusion protein. The same procedures for GST fusion protein purification as described previously for C3-Tat were used. Briefly, a standard curve was first set up to obtain a relationship between known amounts of C3-Tat and

amounts of ADP-ribosylated RhoA. Known amounts of C3-Tat were obtained by serial dilution of freshly purified C3-Tat stock in the same HEPES buffer as that used in the release studies, to a final volume of 50 µl. To each tube containing a known amount of C3-Tat, 150 µl of a solution containing 400 ng RhoA, 8 µM β-NAD (98% free acid, Roche), 5 mM $MgCl_2$ and 1 mM DTT was added. This mixture was incubated at 37°C for 2 hours. 10 µl of the reaction mixture was subjected to Western blot detection with anti-RhoA antibody (1:500 dilution). The immunoreactivity signal was quantified by densitometry using a chemiluminescent imaging system (ChemiGenius2, Syngene, Maryland, USA). The extent of ADP-ribosylation was calculated using equation 3 and plotted against known amounts of C3-Tat to obtain the standard curve (Fig. 6).

$$\text{Extent of ADP-ribosylation (\%)} = \frac{\text{densitometric units of ADP-ribosylated RhoA}}{\text{densitometric units of input RhoA}} \times 100\% \quad (3)$$

To determine the proportion of C3-Tat that remained active after being released from microspheres, 50 µl of medium containing released C3-Tat from each time point was incubated with 150 µl of a solution containing 400 ng RhoA, 8 µM β-NAD (98% free acid, Roche), 5 mM $MgCl_2$ and 1 mM DTT, for 2 hours at 37°C. Western blot was performed with the same conditions as for the standards. The extent of ADP-ribosylation was determined as described above, using equation 3. From the standard curve (Fig. 6), the corresponding amount of active C3-Tat present in the release sample was determined. Comparing this value with the total amount of C3-Tat actually present in the release sample (as determined previously by ELISA) gives an indication of the proportion of

biologically active C3-Tat in each release sample (equation 4).

$$\text{Percentage of C3-Tat that remains active after being released (\%)} = \frac{\text{Amount of active C3-Tat in release sample}}{\text{Total amount of C3-Tat in release sample}} \times 100\% \quad (4)$$

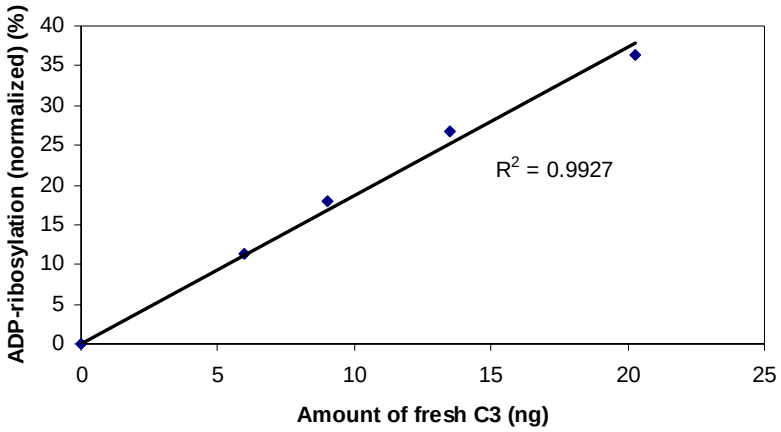

Fig. 6: Standard curve obtained by measuring the extent of ADP-ribosylation for given amounts of freshly purified C3-Tat. The standard curve was subsequently used to determine the amount of biologically active C3-Tat present in release samples.

CHAPTER THREE

RESULTS AND DISCUSSION

3.1. Purification of recombinant C3-Tat

The DNA expression construct (Fig. 7) for C3-Tat was obtained by the addition of Tat and HA sequences to the amino terminal of C3 using recombinant DNA techniques. Tat is a protein transduction domain which has been shown to increase cellular uptake of C3, while the HA epitope tag was added so that C3 can be detected by anti-HA antibodies in Western blots.

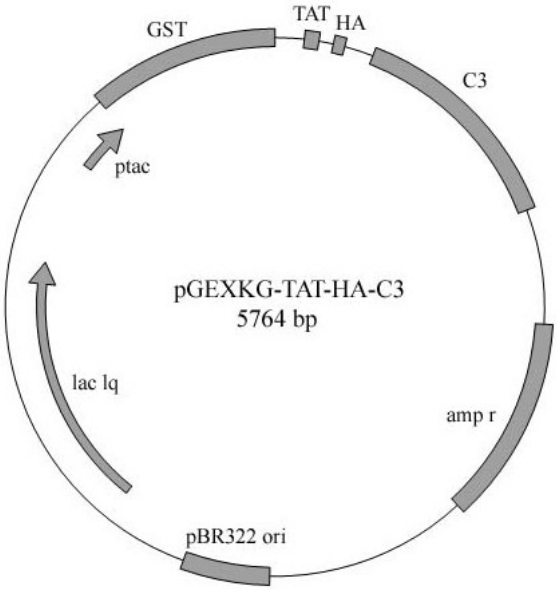

Fig.7: Schematic representation of the expression construct for C3-Tat.

Upon expression of this construct in *E.coli* cells and purification by affinity chromatography, the Tat-HA-C3 protein was obtained as a fusion with GST (Fig. 8). Subsequent cleavage by thrombin protease at its recognition site situated between GST and Tat-HA-C3 produced the purified Tat-HA-C3 protein (thereafter referred to as C3-Tat). The purity and molecular weight of the GST fusion protein before and after cleavage was confirmed by Coomassie staining of SDS-PAGE gel (Fig. 9) and by Western blot (Fig. 10). The cleaved C3-Tat protein was later encapsulated in microspheres.

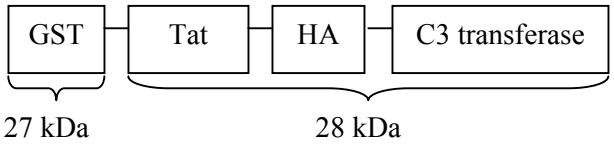

Fig. 8: Schematic representation of the GST-Tat-HA-C3 fusion protein purified from *E.coli* cell lysates.

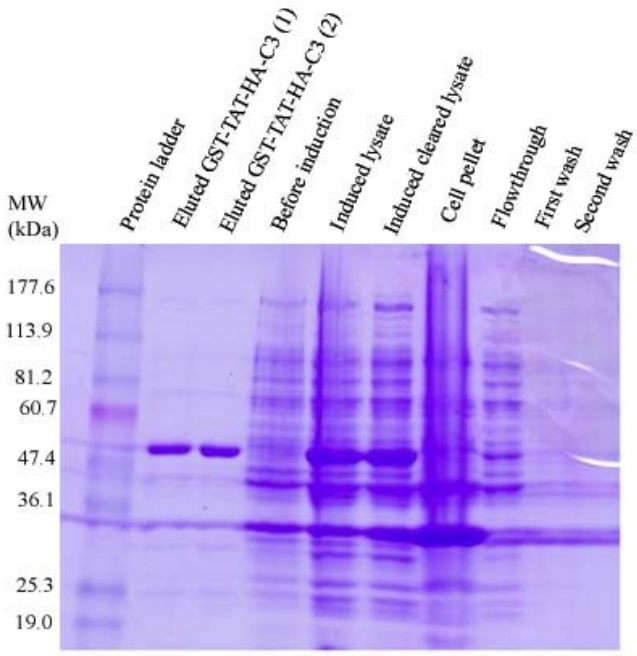

Fig.9: SDS-PAGE gel stained with Coomassie blue showing protein samples from various steps in the GST purification process. The GST-Tat-HA-C3 fusion protein is detected as a 56 kDa band in the gel (Eluted GST-Tat-HA-C3 (1) and (2)).

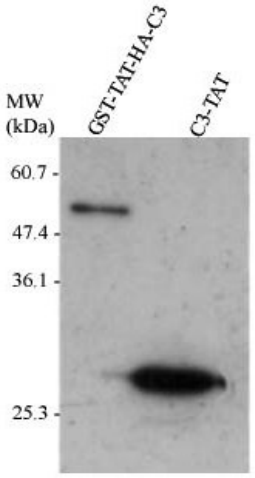

Fig. 10: Western blot of purified GST-Tat-HA-C3 and C3-Tat protein (after thrombin cleavage) probed with anti-HA and anti-rabbit-HRP antibodies. C3-Tat protein is detected as a 28 kDa protein.

3.2. Biological efficacy of purified recombinant C3-Tat

The ability of recombinant C3-Tat and unmodified C3 to enter cells was determined by immunocytochemistry (section 3.2.1), while the ability of the proteins to ADP-ribosylate RhoA intracellularly was determined by Western blot (section 3.2.2).

3.2.1. Cellular uptake of C3-Tat

To study the cellular permeability of C3-Tat (containing both the HA epitope and the Tat peptide) and unmodified C3 (containing HA epitope but not the Tat peptide), fibroblast cells were treated with the purified proteins and immunostained with anti-HA and Alexa Fluor 488 antibodies. In Fig. 11, no intracellular staining was observed when cells were treated with unmodified C3, but staining was observed when cells were treated with C3-Tat. This is consistent with the work of other researchers [27], confirming the increased permeability of C3-Tat proteins at low concentrations.

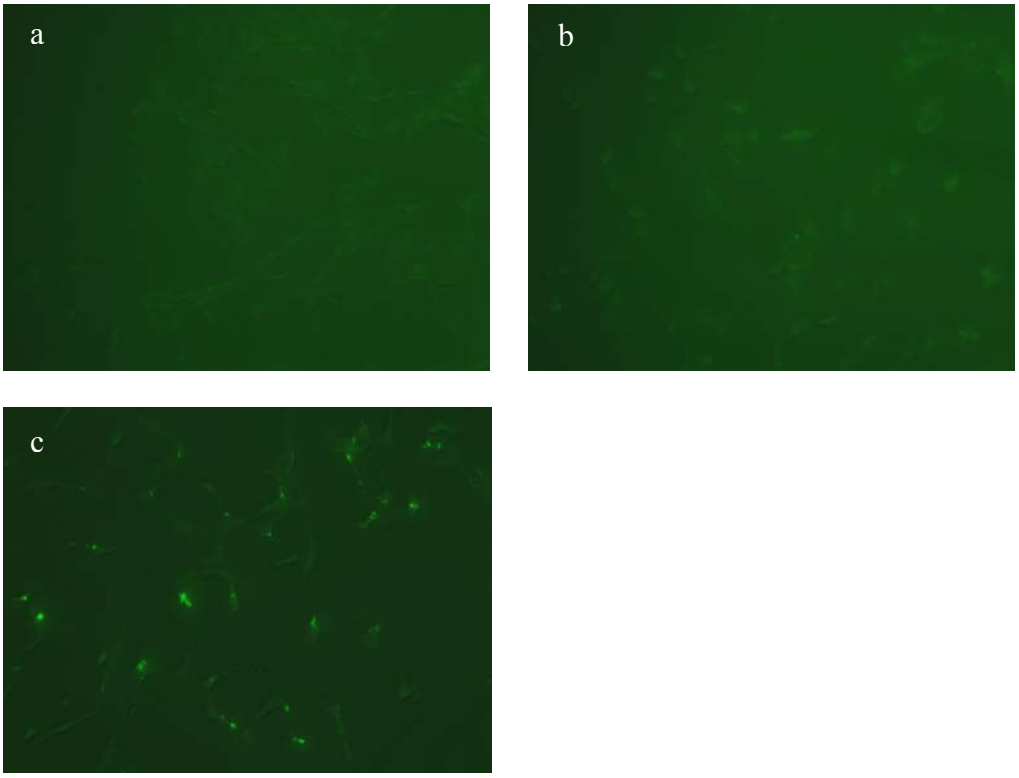

Fig. 11: Efficiency of purified C3-Tat uptake into NIH3T3 fibroblast cells. NIH3T3 cells were incubated with medium containing (a) no added C3, (b) 10 µg/ml unmodified C3, or (c) 10 µg/ml C3-Tat for 24 hours and immunostained with an anti-HA antibody, followed by anti-rabbit Alexa Fluor 488 antibody. The cells were viewed at 200× magnification.

3.2.2. *In vivo* biochemical activity of C3-Tat

ADP-ribosylation of RhoA causes RhoA to migrate with a larger apparent molecular weight on SDS-PAGE gel [74]. To ensure that the purified C3-Tat has the ability to ADP-ribosylate RhoA intracellularly, the electrophoretic mobility of RhoA in fibroblast cells treated with the enzyme or with culture medium alone as a control was examined by Western blot.

A Western blot of cell lysates with anti-RhoA antibody (Fig. 12) clearly shows an upshift in molecular weight of the 22 kDa RhoA upon treatment with 5 µg/ml C3-Tat (lanes 1, 4). Untreated control cells (lane 5) showed no apparent ribosylation of RhoA.

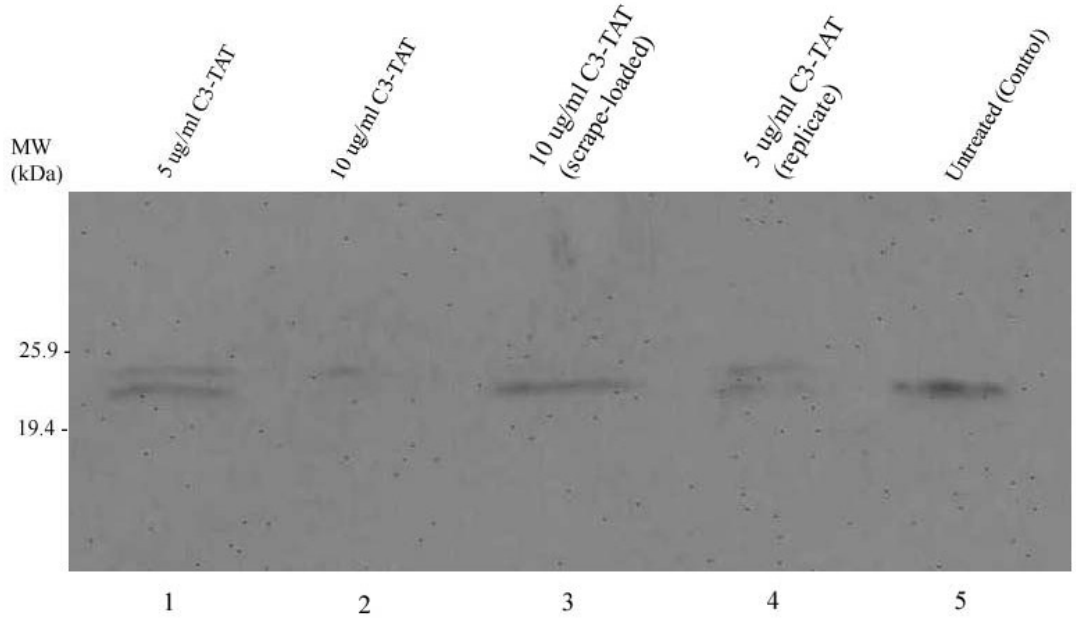

Fig. 12: Intracellular activity of purified C3-Tat. NIH3T3 cells were incubated in medium containing 5 µg/ml C3-Tat (lanes 1 and 4) or 10 µg/ml C3-Tat (lane 2) or no added C3-Tat (control, lane 5) for 24 hours at 37°C. It should be noted that for the samples in the described lanes, C3-Tat was simply added to the medium without any physical disruption to the cells. Western blot of cell lysates was performed with anti-RhoA and anti-mouse-HRP antibodies.

3.3. Microencapsulation of C3-Tat in PLGA microspheres

3.3.1. Physical characteristics of PLGA microspheres encapsulating C3-Tat

To identify the composition of polymers that provides a gradual and persistent release of C3-Tat, the protein was encapsulated in various blends of capped and uncapped PLGA. The physical characteristics of C3-Tat microspheres were tabulated in Table 2 and scanning electron photomicrographs of representative microspheres from each formulation were shown in Fig. 13. All the formulations except 0/100 produced microspheres that are spherical in shape, with smooth and slightly porous surfaces (Fig. 13 A-D). In contrast, the 0/100 microspheres showed rough surfaces and a greater level of surface porosity (Fig. 13 E). The internal microstructure of all the microspheres consisted of spherical pores (Fig. 13 F-J). The degree and distribution of internal porosity appears to be consistent regardless of microsphere formulation. Size of microspheres, however, was apparently independent of the polymer formulations. Mean diameter of the microspheres falls in the range of 74-85 μm. The encapsulation efficiency of the microspheres was consistently above 80%.

Table 2: Characteristics of microspheres.

Microsphere formulation (Capped/uncapped PLGA)	Microsphere size [a] (μm)	Encapsulation efficiency [b] (%)
100/0	83 ± 22	84.3 ± 0.5
70/30	85 ± 26	80.4 ± 2.3
50/50	76 ± 16	87.0 ± 1.3
30/70	75 ± 16	84.8 ± 1.6
0/100	74 ± 18	82.5 ± 2.0

[a] Values are given as mean ± standard deviation of 100 representative microspheres in each formulation

[b] Values are mean ± standard deviation of 3 measurements for each formulation.

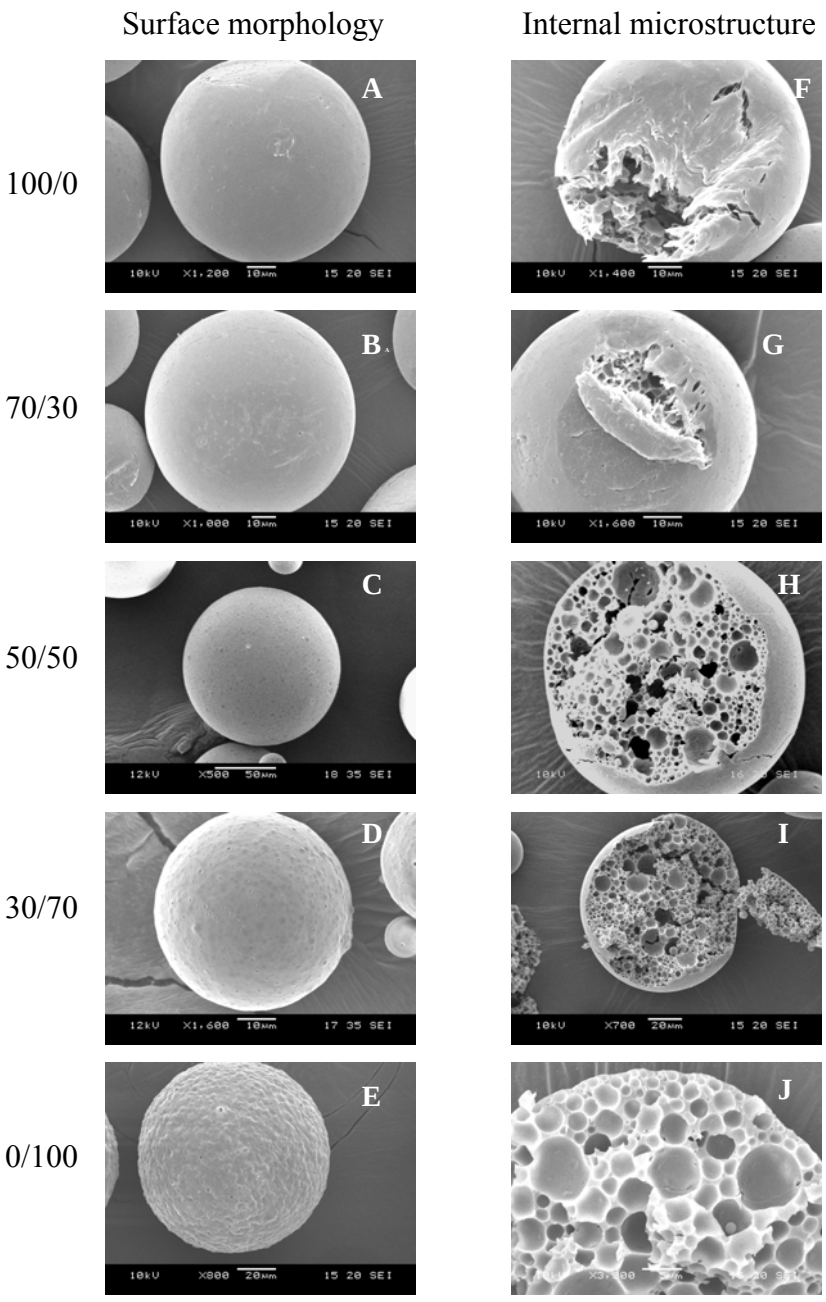

Fig. 13: SEM images of representative microspheres prepared from 100/0, 70/30, 50/50, 30/70 and 0/100 capped/uncapped PLGA. A-E, surface morphology; F-J, internal microstructure.

3.3.2. Protein release characteristics of C3-Tat microspheres

It is known that PLGA microspheres degrade via a random chain scission of the ester linkages in the polymer backbone. The rate of degradation is critically dependent on the physicochemical properties of the polymer and greatly influences the release of the encapsulated drug. Hence, polymers with different functionalities at the end of the polymer chain were investigated in this study. PLGA (50:50) with a hydrophobic ester end-group (capped PLGA) is widely used for protein encapsulation studies, though an initial lag period during which very little or no protein release is usually observed [65, 75]. This type of release characteristic clearly precludes a successful treatment regime. The blending of a PLGA possessing free carboxyl end-groups (uncapped PLGA) with the capped PLGA is expected to compensate for the lag period, ensuring protein release throughout the entire treatment period.

To identify the optimal blending ratio which will provide the desired release profile, the release of C3-Tat from microspheres incubated *in vitro* in a HEPES buffer was monitored. The cumulative release profiles for the microspheres are shown in Fig. 14.

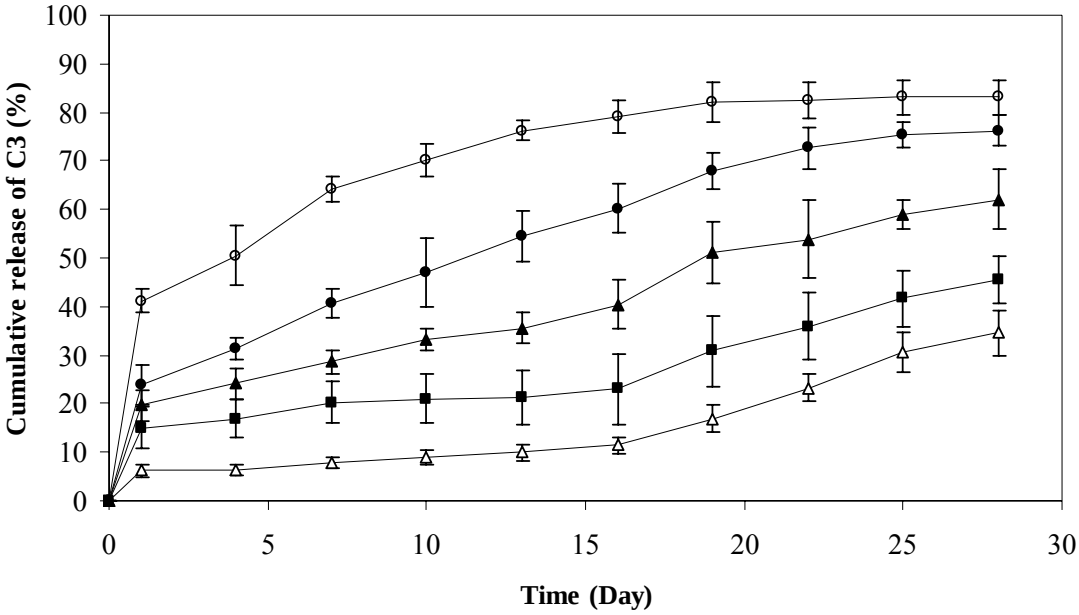

Fig. 14: Release of C3-Tat from microspheres prepared from blends of capped and uncapped PLGA. The proportions of capped PLGA/uncapped PLGA used to prepare the microspheres were: 100/0 (△), 70/30 (■), 50/50 (▲), 30/70 (●) and 0/100 (○). The microspheres were incubated at 37°C in a HEPES buffer, and the amount of C3-Tat released at each time point was determined by ELISA. The amount of C3-Tat released at each time point is expressed relative to the actual total amount of protein initially encapsulated in the microspheres. Error bars represent mean ± standard deviation for n=3.

Microspheres containing 100% capped PLGA (100/0) exhibited less than 10% burst release within 24 hours, followed by a lag phase of about 19 days, during which almost no protein was released. Release gradually increased after this time and by day 28, only 30% of encapsulated C3-Tat was released. In contrast, the release of C3-Tat from uncapped PLGA microspheres (sample 0/100) was characterized by an initial burst of

40% within the first 24 hours of incubation, followed by a subsequent average daily release rate of about 2.5% until a plateau value of about 80% encapsulated protein being released by day 28. The initial burst can be attributed to the immediate dissolution and release of the proteins near the surface of the microspheres [76]. It is likely that the rough surface feature of the 0/100 formulation confers a bigger surface area exposed to the aqueous environment, thereby increasing the rate and extent of initial hydration of the microspheres, leading to the large initial burst [76].

The blends of various percentage of capped and uncapped PLGA exhibit intermediate release profiles between the two extremes, which is consistent with the observations published by other researchers [58, 59]. The initial lag period was gradually eliminated as the proportion of uncapped polymer in the microspheres was increased. Sample 70/30 showed a lag of about 16 days while sample 50/50 had a lag period of 13 days. In particular, the lag period was completely eliminated in sample 30/70, which showed an initial burst of 25% and subsequently an average daily release rate of 2.3% (Fig.15). This translates to an average daily release of 3.0 ng/day/mg over a period of almost a month.

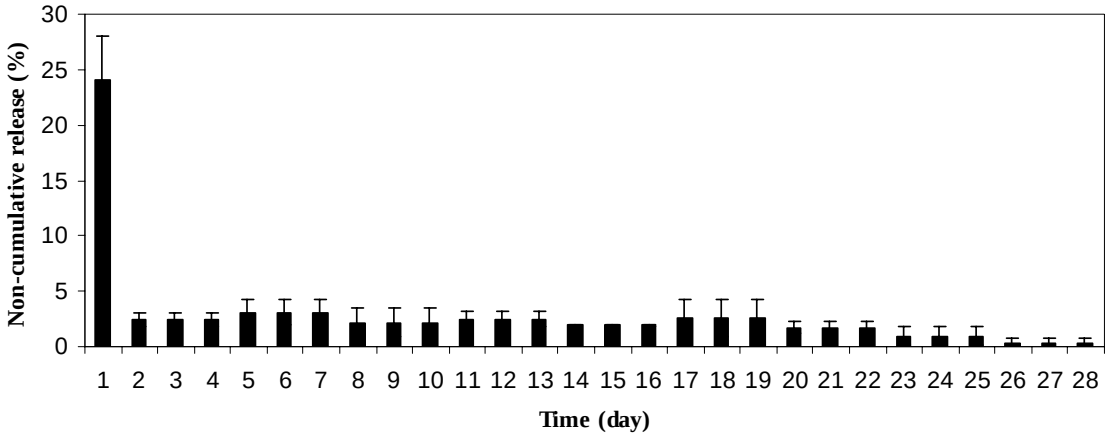

Fig. 15: Non-cumulative release of C3-Tat from 30/70 capped/uncapped PLGA microspheres incubated at 37°C in a HEPES buffer. The amount of C3-Tat released at each time point is expressed relative to the actual total amount of protein initially encapsulated in the microspheres. Error bars represent mean ± standard deviation for n=3.

3.3.3 Changes in physical characteristics of C3-Tat microspheres during degradation *in vitro*

Release of protein drugs from microspheres occurs by diffusion through interconnected channels created by polymer degradation and erosion. The effect of addition of uncapped PLGA on the degradation and erosion characteristics of the microspheres, and hence the release of C3-Tat, was assessed by monitoring the molecular weight (Figs.16, 17), mass (Fig.18) and morphology (Fig.19) of the microspheres incubated in HEPES buffer. Other features of the microspheres and experimental conditions which could affect degradation rate were kept constant across the different blends. This allows the effect of endgroup chemistry on the degradation and erosion of microspheres to be studied. During

production of all of the microsphere blends, the double emulsion procedures and formulation parameters were kept constant. Therefore, the resulting microsphere sizes and level of internal porosity were consistently similar across the different blends. Similarly, the *in vitro* release conditions were kept constant for all the blends.

Fig. 16 shows that sample 100/0 had an initial molecular weight of 32 kDa which decreased by less than 3% during the first 3 weeks. This slow rate of degradation (degradation rate constant of -0.0107 day^{-1}, Table 3) explains the lack of significant mass loss (Fig.18) during the first 3 weeks. SEM images (Fig. 19a) also showed no morphological changes in the first three weeks. After this time, an increase in roughness and porosity at the surface of the microspheres was observed. The microspheres still retain their spherical shape. The lack of any significant degradation during the first three weeks of incubation accounts for the initial lag period during which very little C3-Tat was released. The increase in porosity after 3 weeks coincided with an increase in the rate of C3-Tat release. The overall triphasic (S-type) shape of the release profile is consistent with that typically seen for protein drugs encapsulated in capped PLGA [53, 54].

In contrast, the 0/100 microspheres exhibited different degradation characteristics. It has been shown that 15 kDa represents the critical value for PLGA at which oligomeric degradation products become water soluble, and hence the point at which erosion initiates [58]. Microspheres prepared from uncapped PLGA (sample 0/100) exhibited an initial molecular weight of 11 kDa which is already below the critical point. It was observed that the molecular weight decreased by almost 30% within the first week of incubation

(Fig. 16). Together with the continuous loss of mass of the microspheres (Fig. 18) from the start of incubation, it is likely that PLGA degradation products are solubilised immediately, thereby facilitating microsphere erosion. This is supported by morphological analyses of microspheres, which show deformation and increased porosity within the first week of incubation (Fig. 19e). The microspheres became increasingly fragmented and porous with time. The continuous erosion from the start of incubation coincided with the continuous release of C3-Tat upon immersion in the aqueous medium.

When uncapped PLGA was blended with the capped polymer in varying proportions, the degradation kinetics of the resulting microspheres were altered. Increasing the proportion of uncapped polymer led to lower initial molecular weights, higher rates of degradation and mass loss as well as faster progression of pore formation and microsphere fragmentation. For all the blends, the point in time at which significant mass loss began coincided with an increased rate of release of C3-Tat. Cross section of the 30/70 microspheres after 7 days of incubation (Fig. 20) showed the presence of newly formed internal pores on the walls of existing pores, hence leading to the formation of interconnected channels within the matrix. Formation of new pores was also observed in the 50/50 and 70/30 microspheres at a later time (after 14 days of incubation, data not shown). There is evidence that even in a homogenous mixture of two polymers, gelling and solidification of the polymers occurs separately [77]. In this case, it can be hypothesized that the more hydrated domains of the uncapped polymer within the microsphere matrix degrade and erode first, forming new pores and enlarging existing ones. These form interconnected channels through which polymer degradation products

and C3-Tat diffuse into the medium. The formation of such interconnected channels in the 30/70 microspheres early in the incubation period explains the sustained, constant release of C3-Tat throughout the one month period.

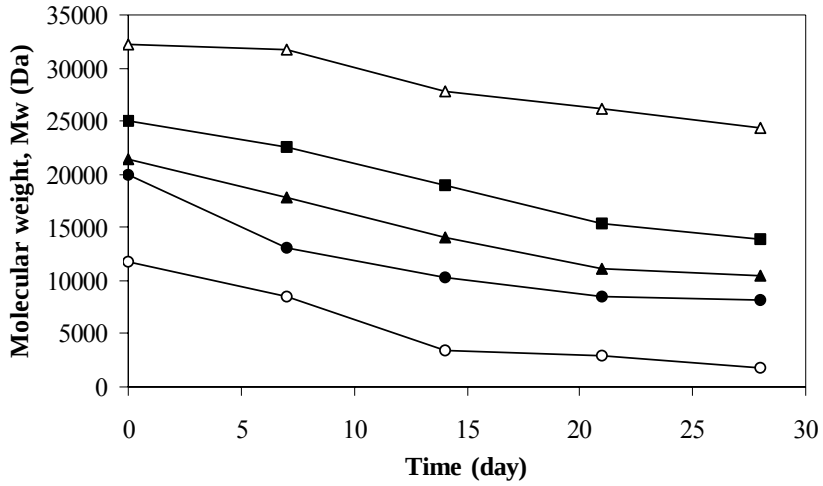

Fig. 16: Change in weight-average molecular weight of microspheres incubated at 37°C in HEPES buffer. The proportions of capped PLGA/uncapped PLGA used to prepare the microspheres were: 100/0 (△), 70/30 (■), 50/50 (▲), 30/70 (●) and 0/100 (○). M_w values were determined for only one of three sets of each of the microsphere blends.

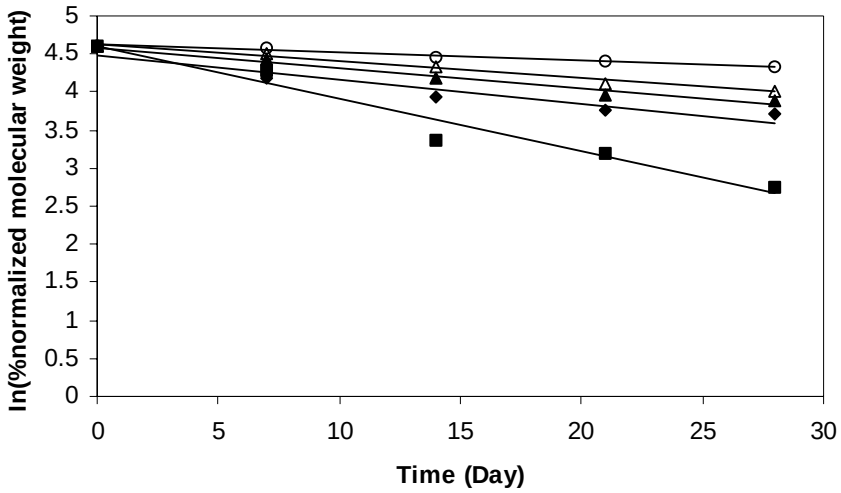

Fig. 17: Semilog plots of normalized weight-average molecular weight versus time for the following samples: 100/0 (○), 70/30 (△), 50/50 (▲), 30/70 (◆) and 0/100 (■). The weight-average molecular weight (M_w) at each time point was normalized to the initial weight-average molecular weight (M_{wo}). The line is a linear least-squares fit to the data. The degradation rate constant was determined from the slope of each line.

Table 3: *In vitro* degradation kinetics of the microspheres.

Formulation	Degradation rate constant [a] (day^{-1})	Correlation coefficient, r^2
100/0	-0.0107	0.9597
70/30	-0.0224	0.9847
50/50	-0.0272	0.9734
30/70	-0.0316	0.9108
0/100	-0.0688	0.9583

[a] This is the slope of the semilog plot of normalized molecular weight versus time

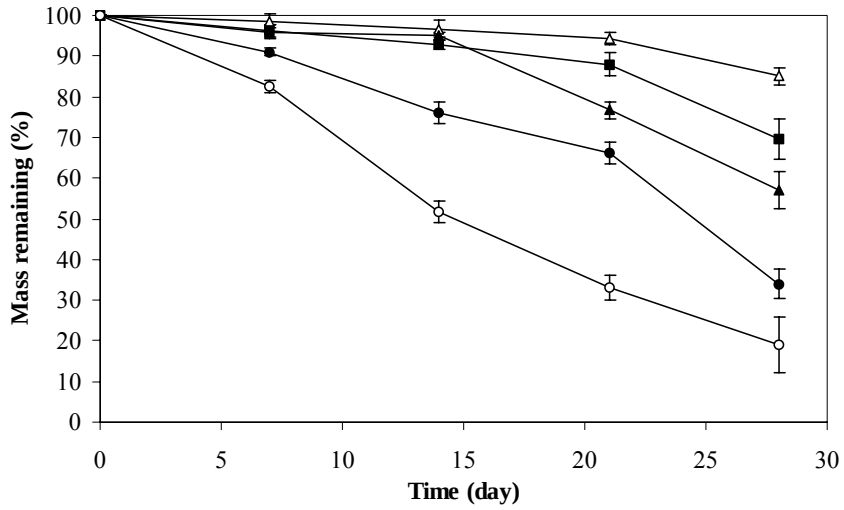

Fig. 18: Mass loss profile of microspheres incubated at 37°C in HEPES buffer. The compositions of capped PLGA/uncapped PLGA used to prepare the microspheres were: 100/0 (△), 70/30 (■), 50/50 (▲), 30/70 (●) and 0/100 (○). Mass remaining at each time point was calculated by comparing the mass at a given time point to the initial mass. Error bars represent mean ± standard deviation for n=3.

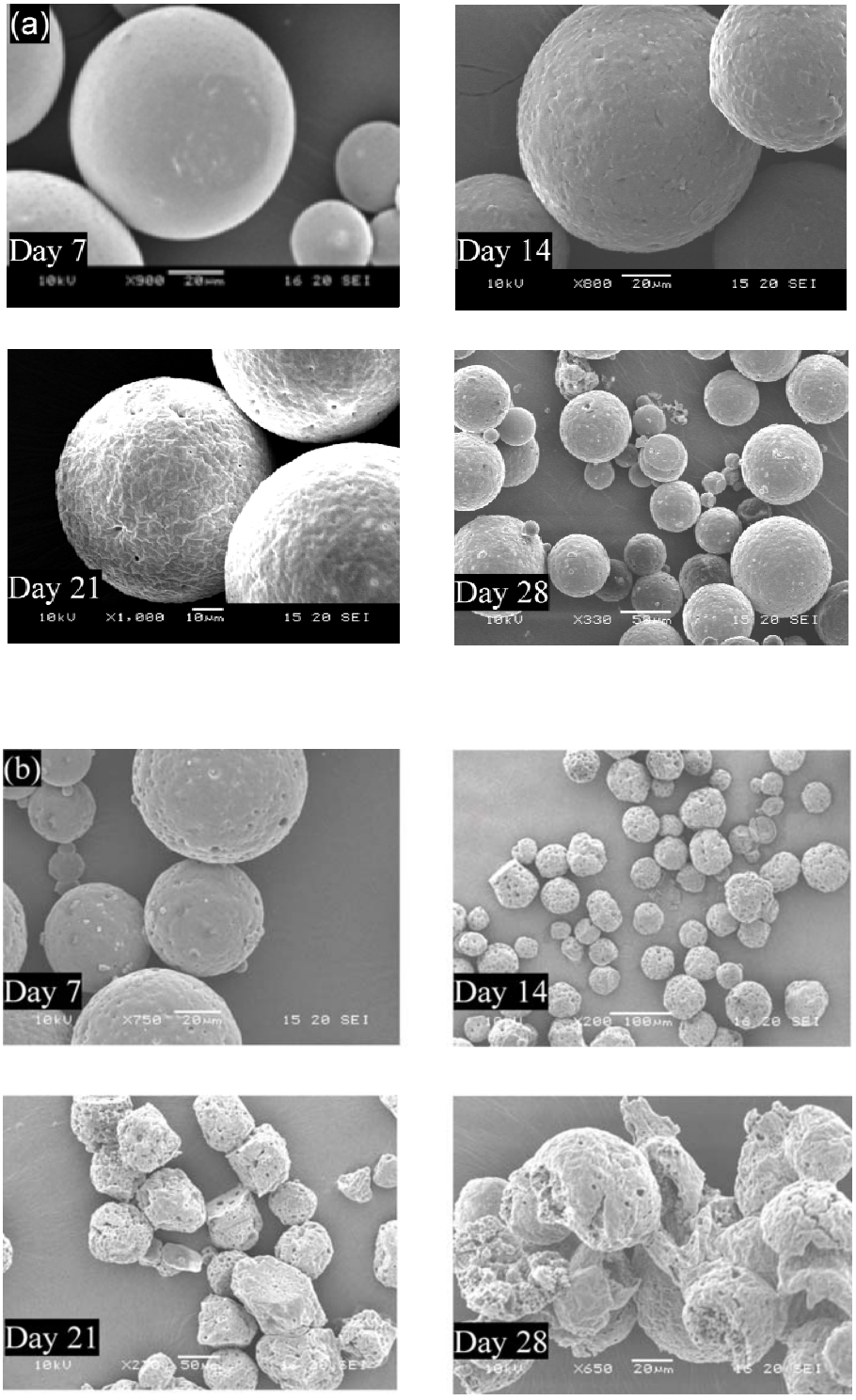

Fig. 19: SEM images of microspheres prepared from (a) 100/0, (b) 70/30, (c) 50/50, (d) 30/70 and (e) 0/100 capped/uncapped PLGA, at various time points, after incubation in HEPES buffer at 37°C.

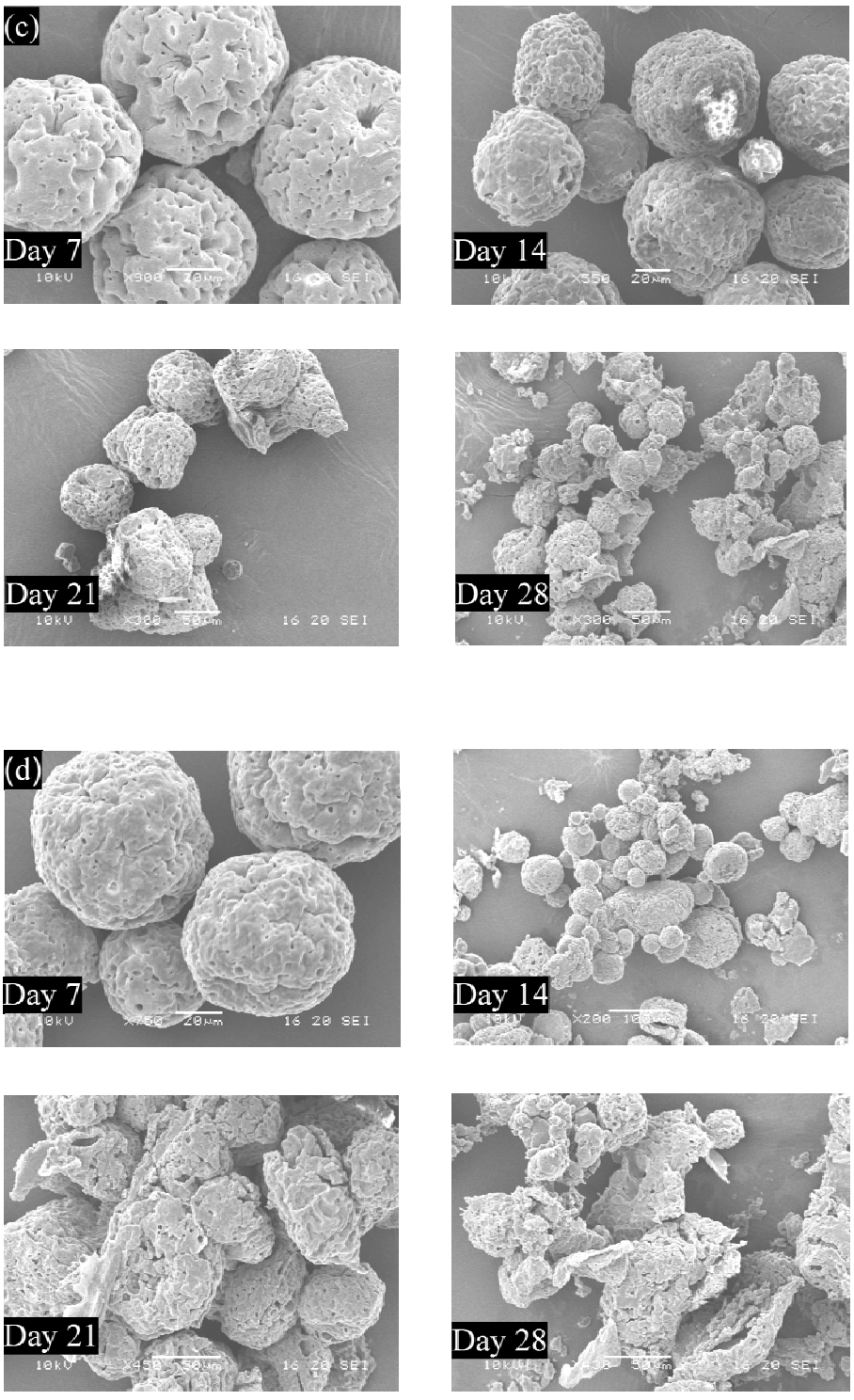

Fig. 19 (Continued)

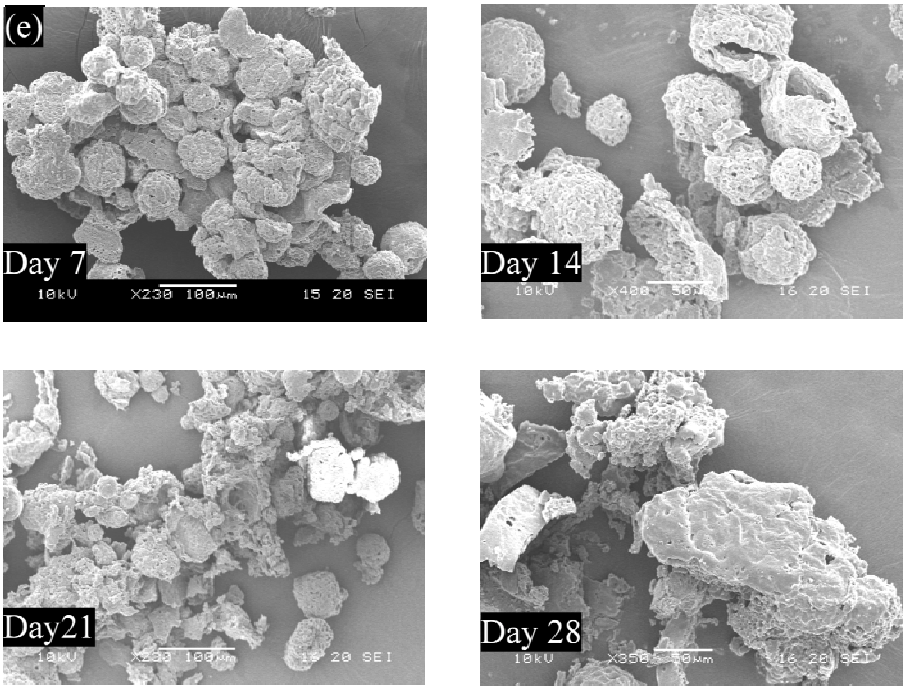

Fig. 19 (Continued)

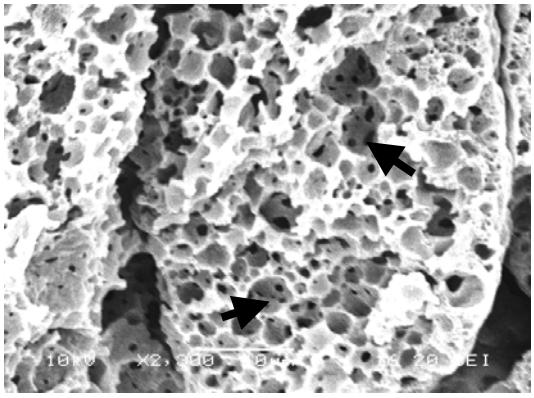

Fig. 20: The internal pore structure of 30/70 microspheres after 7 days of incubation in HEPES buffer. Arrows indicate some of the newly formed pores on the walls of the existing pores.

3.3.4. Bioactivity of released C3-Tat

The activity of C3-Tat released from PLGA microspheres over time was examined by measuring its catalysis of ADP-ribosylation of recombinant RhoA with an *in vitro* assay. By interpolation of the standard curve (Fig. 6), the amount of active C3-Tat present in each sample at each time point was determined, and expressed as a percentage of the total C3-Tat released (as detected by ELISA) (Fig. 21). The biological activity of C3-Tat was maintained in the 30/70 microspheres for at least 19 days, as at least 40% of the released C3-Tat during this period was found to be active. After 19 days, the activity of C3-Tat appears to drop drastically.

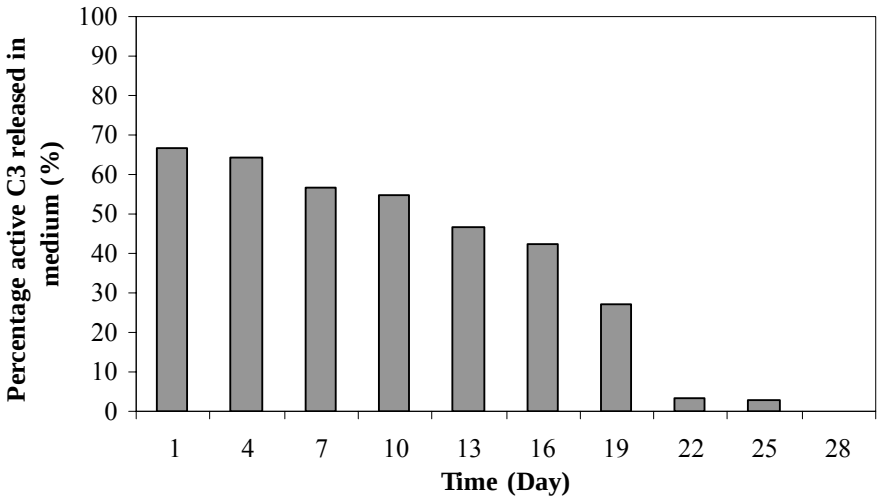

Fig 21: Percentage of C3-Tat that remains active after being released from the 30/70 microspheres. The amount of active C3-Tat in each release sample at every time point was determined by an *in vitro* assay in which C3-Tat was incubated with recombinant RhoA and β-NAD in a suitable buffer. ADP-ribosylation of RhoA was detected as an increase in molecular weight of RhoA on a Western blot. The amount of active C3-Tat at each time point is expressed as a percentage of the total C3-Tat released at that time point as detected by ELISA. Each data point is an average of measurements from two sets of microspheres.

3.4. Discussion

In this study, the approach of blending polymers with hydrophobic ester end-groups (capped PLGA) and hydrophilic carboxyl end-groups (uncapped PLGA) for controlling the release rate of encapsulated C3 was investigated. As the molecular weight of blends was found to be different, the observed differences in degradation rate and therefore release rate of the blends cannot be attributed entirely to the addition of uncapped PLGA. However, a study comparing microspheres prepared from 12 kDa capped and uncapped 50:50 PLGA respectively reported slower release of protein from the capped PLGA microspheres [78]. It was proposed that the higher hydrophilicity of the uncapped PLGA gave rise to a faster degradation rate. Indeed, other studies have found that PLGA molecular weight had a much smaller effect than the end group on the degradation rate constant of microspheres [69]. In the same study [69] it was found that uncapped PLGA degraded faster because of the catalysis of ester bond hydrolysis due to the larger number of free carboxyl end groups, and also because of larger rate of water uptake. Therefore, the increase in degradation rate and release rate observed in our study when the proportion of uncapped PLGA is increased is likely to be due mainly to the effect of the free carboxylic endgroups, rather than the drop in molecular weight.

For every blend, an increased rate of release of C3-Tat was consistently observed at the point in time when physical erosion of the microspheres occurred. This is an indication that the release of protein from the microspheres in this study is erosion-controlled. The optimal blending ratio which resulted in continuous release immediately upon immersion in a buffer solution was found to be 30/70 ratio of capped/uncapped PLGA. After an

initial burst of 25%, an average daily protein release of 3.0 ng/day/mg microspheres was observed. The initial burst could be advantageous in this application, as there is evidence that the application of a large dose of C3 to injured CNS tissue within the first 24 hours after injury leads to increased neuroprotection [16]. Neuronal survival in the early stages of injury is important for successful functional recovery. After the burst, maintenance of C3 release at a constant level would ensure continual supply of the protein necessary for long-distance axonal regeneration of the injured neurons.

Proteins are known to be susceptible to denaturation, aggregation and adsorption at interfaces, all of which affects their conformation in solution, and in turn their biological activity. It is known that when microspheres encapsulating proteins are prepared by the w/o/w double emulsion method, the protein is especially susceptible to adsorption and denaturation at the water/organic solvent interface [78, 79]. The other major factor contributing to instability of the encapsulated protein is the *in vitro* release conditions [80, 81]. As such, the activity of C3-Tat released from the incubated microspheres at various time points was also studied.

The C3-Tat released on the first day provides an indication of the effect of the microencapsulation processing steps on the integrity of the protein, as the protein would not have been exposed to the medium for extended periods of time. This study has shown that 70% of the released C3-Tat on the first day of incubation is still biologically active. This value indicates that the method of stabilization of C3 (i.e. addition of PEG to the inner aqueous phase) during the encapsulation procedure can be further optimized. It is

likely that PEG was not completely effective in protecting C3. It is speculated that it is most likely the primary emulsification step which poses the most harm to C3. The use of other excipients reported to prevent emulsification-induced denaturation and degradation of proteins should be investigated. Such excipients include osmolytes, such as trehalose and mannitol, which acts by shielding proteins from the organic solvent by preferential hydration [78]. In addition, the type of organic solvent can also influence protein stability. Compared to the more hydrophobic dichloromethane, ethyl acetate has been reported to induce less denaturation of proteins [82].

The observed steady drop in activity of C3-Tat over the subsequent days is similar to that reported by other researchers in similar studies where microspheres were suspended in a fixed volume of buffer in a closed container [80, 83]. The loss of protein integrity during incubation of microspheres *in vitro* has been attributed to protein aggregation following initial rehydration of the microspheres, to protein adsorption to the polymer, or to the acidification of the release medium by PLGA degradation products [81, 84]. In this study, the use of HEPES buffer (which has larger buffer capacity than phosphate-buffered saline, PBS) and replacement of buffer every 3 days, led to maintenance of release medium at pH 7 throughout the study period (data not shown). Although the pH measured was of the buffer outside of the microspheres, it is speculated that the internal environment within the microspheres will not be very different, as the high porosity of the microspheres allows for rapid diffusion of degradation products into the surrounding medium. As such, the soluble degradation products of PLGA consisting of monomers and oligomers may be compromising the stability of C3-Tat in other ways. For example, the

degradation products may exert co-solvent effects on C3-Tat, i.e. their presence may decrease conformational stability [80]. Prolonged exposure of C3-Tat in solution at 37°C may also contribute to its instability [81].

After 19 days of incubation, the amount of active C3-Tat in the medium drops drastically, though the protein is still detectable by ELISA. This is an indication that after a long period of incubation, C3-Tat still maintains its immunoreactivity (i.e. its recognition by antibodies) but loses much of its biological activity. There is evidence from previous studies [84 – 87] that antigen reactivity may not be strictly related to biological activity because a protein may lose biological activity without losing its epitopes reactivity. The drastic drop in activity after about 19 days of incubation may be explained by the increasing porosity and hydration of microspheres with time, which expose C3-Tat in microspheres to the environmental stresses described above.

The *in vitro* release study conditions are not representative of the actual *in vivo* situation, where the polymer degradation products may be readily cleared away [67]. It is not possible to mimic exactly the *in vivo* environmental conditions in an *in vitro* setup. Despite the limitations of *in vitro* studies, they are still useful as a screening tool during optimization of microsphere formulations. As such, it is worthwhile optimizing the *in vitro* conditions. Variables in the release medium which can be optimized include pH, buffer species, ionic strength and salt concentration. There is evidence that the buffer components in the release medium make a big difference in retaining protein activity during prolonged incubation at 37°C [ref 80, 81].

It should be noted that while *in vitro* studies provide a simple preliminary method to identify microsphere formulations which give the desired release profile and protein stability, such studies may not accurately assess the biological efficacy of the microspheres. Further *in vivo* studies in rodent models are necessary to assess and confirm the biological efficacy of C3-Tat in PLGA microspheres.

CHAPTER FOUR

CONCLUSIONS AND RECOMMENDATIONS

4.1. Conclusions

The objective of this study was to assess the feasibility of encapsulating recombinant C3-Tat protein within PLGA microspheres to achieve a gradual and localized release of active protein over an extended period of time. The degradation rate of the microspheres can be controlled by the blending ratio of capped and uncapped PLGA. The release of C3-Tat from the microspheres was controlled by matrix erosion, where interconnected channels facilitated diffusion of the protein from the matrix. It was demonstrated that the optimal blending ratio giving rise to microspheres fulfilling the requirement of continuous release for at least one month, was a 30/70 ratio of capped/uncapped PLGA. In this formulation, an average daily C3-Tat release of 3.0 ng/day/mg microspheres was observed for a period of one month.

While this study has demonstrated that the release characteristics of the microspheres are suitable for our target application, the activity levels of released C3-Tat could not be accurately assessed, given the instability of the protein in the *in vitro* release conditions. 70% of the released C3-Tat on the first day of incubation was found to be active. At least 40% of C3-Tat biological activity was maintained in the 30/70 microspheres for 19 days. After 19 days, the activity of C3-Tat dropped to very low levels. These results indicate that the method of stabilization of C3 during the encapsulation procedure and release

studies can be further optimized. Further characterization of the C3-Tat microspheres in rodent models of spinal cord injury is also necessary for confirmation of its biological activity.

4.2. Recommendations for future work

A comprehensive formulation study for C3-Tat should be conducted, where different stabilization methods are systematically tested to identify one that will ensure that C3 retains its activity during the emulsification process and during *in vitro* incubation.

To ensure that microspheres remain localized at the required site in the spinal cord, it is proposed that the C3-Tat microspheres be suspended in a gel matrix, e.g. collagen or fibrin matrix. In this way the axonal growth supporting properties of these gels can also be exploited. The release characteristics of C3-Tat may be altered due to the presence of the gel, and this aspect must be further characterized.

REFERENCES

[1] C.E. Hulsebosch, Recent advances in pathophysiology and treatment of spinal cord injury, Adv. Physiol. Educ. 26 (2002) 238-255.

[2] J.W. Mcdonald, C. Sadowsky, Spinal cord injury seminar, Lancet 359 (2002) 417-425.

[3] R.J. McKeon, R.c. Schreiber, J.S. Rudge, J. Silver, Reduction of neurite outgrowth in a model of glial scarring following CNS injury is correlated with the expression of inhibitory molecules on reactive astrocytes, J. Neurosci. 11 (1991) 3398-3411.

[4] R.A. Asher, D.A. Morgenstern, P.S. Fidler, K.H. Adcock, A. Oohira, J.E. Braistead, J.M. Levine, R.U. Margolis, J.H. Rogers, J.W.Fawcett, Neurocan is upregulated in injured brain and in cytokine-treated astrocytes, J. Neurosci. 20 (2000) 2427-2438.

[5] R.J. Pasterkamp, F. De Winter, R.J. Giger, J. Verhaagen, Role for semaphorin III and its receptor neuropilin-1 in neuronal regeneration and scar formation? Prog. Brain Res. 117 (1998) 151-170.

[6] M.E. Schwab, P. Caroni, Rat CNS myelin and a subtype of oligodendrocytes in culture represent a non-permissive substrate for neurite growth and fibroblast spreading, J. Neurosci. 8 (1988) 2381-2393.

[7] R. Prinjha, S.E. Moore, M. Vinson, S. Blake, R. Morrow, G. Christie, et al., Inhibitor of neurite outgrowth in humans, Nature 403(2000) 383-384.

[8] K.C. Wang, V. Koprivica, J.A. Kim, R. Sivasankaran, Y. Guo, R.L. Neve, Z. He, Oligodendrocyte-myelin glycoprotein is a Nogo receptor ligand that inhibits neurite outgrowth, Nature 417 (2002) 941-944.

[9] L. McKerracher, S. David, D.L. Jackson, V. Kottis, R.J. Dunn, P.E. Braun, Identification of myelin-associated glycoprotein as a major myelin-derived inhibitor of neurite outgrowth, Neuron 13 (1994) 805-811.

[10] A. Sandvig, M. Berry, L.B. Barrett, A. Butt, A. Logan, Myelin-, reactive glia-, and scar-derived CNS axon growth inhibitors: Expression, receptor signaling and correlation with axon regeneration, Glia 46 (2004) 225-251.

[11] B.J. Dickson, Rho GTPases in growth cone guidance, Curr. Opin. Neurobiol. 11 (2001) 103-110.

[12] L. Luo, Rho GTPases in neuronal morphogenesis, Nature Rev. Neurosci. 1 (2000) 173-180.

[13] M. Lehmann, A. Fournier, I.Selles-Navarro, P. Dergham, A. Sebok, N. Leclerc, et al., Inactivation of Rho signaling pathway promotes CNS axon regeneration, J. Neurosci. 19 (1999) 7537-7547.

[14] A.E. Fournier, B.T. Takizawa, S.M. Strittmatter, Rho kinase inhibition enhances axonal regeneration in the injured CNS, J. Neurosci. 23 (2003) 1416-1423.

[15] Z. Jin, S.M. Strittmatter, Rac1 mediates collapsing-1 induced growth cone collapse. J. Neurosci. 17 (1997) 6256-6263.

[16] P. Dergham, B. Ellezam, C. Essagian, H. Avedissian, W.D. Lubell, L. Mckerracher, Rho signaling pathway targeted to promote spinal cord repair, J. Neurosci. 22 (2002) 6570-6577.

[17] U. Laufs, M. Endres, N. Stagliano, S. Amin-Hanjani, D.S, Chui, et al., Neuroprotection mediated by changes in the endothelial actin cytoskeleton, J. Clin. Invest. 106 (2000) 15-24.

[18] T. Trapp, L. Olah, I. Holker, M. Besselmann, C. Tiesler, K. Maeda, K.A. Hossmann, GTPase RhoB: an early predictor of neuronal death after transient focal ischemia in mice, Mol. Cell. Neurosci. 17 (2001) 883-894.

[19] R.J. Ridley, A. Hall, The small GTP-binding protein Rho regulates the assembly of focal adhesions and stress fibres in response to growth factors, Cell 70 (1992) 389-399

[20] E.J. Rubin, M.D. Gill, P.Boquet, M.R. Popoff, Functional modification of a 21-kilodalton G Protein when ADP-ribosylated by exoenzyme C3 of Clostridium botulinum, Mol. Cell. Biol. 8 (1988) 418.

[21] Y. Saito, S. Narumiya, Preparation of Clostridium botulinum C3 exoenzyme and application of ADP-ribosylation of Rho proteins in biological systems, in: K. Aktories (Ed.), Bacterial toxins, Chapman&Hall, Weinhem, 1997, pp 85-92.

[22] M. Green, P.M. Loewenstein, Autonomous functional domains of chemically synthesized human immunodeficiency virus tat trans-activator protein, Cell 55 (1988) 1179-1188.

[23] A.D. Frankel, C.O. Pabo, Cellular uptake of the tat protein from human immunodeficiency virus, Cell 55 (1988) 1189-1193.

[24] S.K. Arya, C. Guo, S.F. Josephs, F. Wong-Staal, Transactivator gene of human T-lymphotropic virus type III, Science 229 (1985) 69-75.

[25] E. Vives, P. Brodin, B. Leblus, A truncated tat basic domain rapidly translocates

through the plasma membrane and accumulates in the nucleus, J. Biol. Chem. 272 (1997) 16010-16017.

[26] S.R. Schwarze, A. Ho, A. vocero-Akbani, S.F. Dowdy, In vivo protein transduction: delivery of a biologically active protein into the mouse, Science 285 (1999) 1569-1572

[27] M. J. Winton, C.I. Dubreuil, D. Lasko, N. Leclerc, L. McKerracher, Characterization of new cell permeable C3-like proteins that inactivate Rho and stimulate neurite outgrowth on inhibitory substrates, J. Biol. Chem. 277 (2002) 32820-32829.

[28] P.A. Dijkhuizen, J.Verhaagen, The use of neurotrophic factors to treat spinal cord injury: advantages and disadvantages of different delivery methods, Neurosci. Res. Commun. 24 (1999) 1-10.

[29] Medtronic, Introduction to intrathecal drug delivery. Available at: http://www.medtronic.com/neuro/paintherapies/pain_treatment_ladder/drug_infusion/drug_drug_deliv.html, Accessed on 27 March 2005.

[30] T. GrandPre, S. Li, S.M. Strittmattter, Nogo-66 receptor antagonist peptide promotes axonal regeneration, Nature 417 (2002) 547-551.

[31] M.S. Ramer, J.V. Priestley, S.B. McMahon, Functional regeneration of sensory axons into the adult spinal cord, Nature 403 (2000) 312-316.

[32] L.L. Jones, M.H. Tuszynski, Chronic intrathecal infusions after spinal cord injury cause scarring and compression, Microsc. Res. Tech. 54 (2001) 317-324.

[33] R.D. Penn, J.S. Kroin, M.M. York, Intrathecal ciliary neurotrophic factor delivery for treatment of amyotrophic lateral sclerosis (phase I trial), Neurosurgery 40 (1997) 94-99.

[34] S.J. Taylor, J.W. Mcdonald III, S.E. Sakiyama-Elbert, Controlled release of neurotrophin-3 from fibrin gels for spinal cord injury, J Control. Release 98 (2004) 281-294.

[35] L.L. Jones, R.U. Margolis, M.H. Tuszynski, The chondroitin sulfate proteoglycans neurocan, brevican, phosphacan, and versican are differentially regulated following spinal cord injury, Exp. Neurol. 182 (2003) 399–411.

[36] A. Buss, K. Pech, D. Merkler, B.A. Kakulas, D. Martin, J. Schoenen, J. Noth, M.E Schwab, G.A. Brook, Sequential loss of myelin proteins during Wallerian degeneration in the human spinal cord, Brain 128 (2005) 356-364.

[37] A.H. Zisch, M.P. Lutolf, J.A. Hubbell, Biopolymeric delivery matrices for angiogenic growth factors, Cardiovasc. Pathol. 12 (2003) 295–310.

[38] P.K. Shireman, B. Hampton, W.H. Burgess, H.P. Greisler, Modulation of vascular cell growth kinetics by local cytokine delivery from fibrin glue suspensions, J. Vasc. Surg. 29 (1999) 852-861.

[39] D.G. Wallacea, J. Rosenblattb, Collagen gel systems for sustained delivery and tissue engineering, Adv. Drug. Deliv. Rev. 55 (2003) 1631– 1649.

[40] S. Li, M. Vert, Biodegradable polymers: Polyesters in: E. Mathiowitz, Encyclopedia of controlled drug delivery, Wiley-Interscience, New York, 1999, pp 71-91.

[41] V.R. Sinha, A. Trehan, Biodegradable microspheres for protein delivery, J. Control. Release 90 (2003) 261-280.

[42] P.A. Lee, Treatment of central precocious puberty with depot lupron, in: G.D. Grave, Sexual precocity: etiology, diagnosis and management, Raven Press, New York, 1993, pp 139-150.

[43] R.A. Jain, The manufacturing techniques of various drug loaded biodegradable poly(lactide-co-glycolide) (PLGA) devices, Biomaterials 21 (2000) 2475-2490.

[44] O.L. Johnson, M.A. Tracy, Peptide and protein drug delivery, in: E. Mathiowitz, Encyclopedia of controlled drug delivery, Wiley-Interscience, New York, 1999, pp 816-833.

[45] X. Li, X. Deng, Z. Huang, In vitro protein release and degradation of poly-dl-lactide-poly(ethylene glycol) microspheres with entrapped human serum albumin: quantitative evaluation of the factors involved in protein release phases, Pharm. Res. 18 (2001) 117-124.

[46] R.C. Mehta, J. Ramasbu, S. Calis, B.C. Thanoo, K. W. Burton, P.P. DeLuca, Biodegradable microspheres as depot system for parenteral delivery of peptide drugs, J. Control. Release 29 (1994) 375-384.

[47] D.T. O'Hagan, J.P. McGee, R. Boyle, D. Gumaer, X-M. Li, B. Potts, C.Y. Wang, W.C. Koff, The preparation, characterization and pre-clinical evaluation of an orally administered HIV-1 vaccine, consisting of a branched peptide immunogen entrapped in controlled release microparticles, J Control. Release 36 (1995) 75-84.

[48] D.Bodmer, T. Kissel, E. Traechslin, Factors influencing the release of peptides and proteins from biodegradable parenteral depot systems, J. Control. Release 21 (1992) 129-138.

[49] T.G. Park, Degradation of poly(dl-lactic acid) microspheres: effect of molecular weight, J. Control. Release, 30 (1994) 161-173.

[50] G. Crotts, T.G. Park, Preparation of porous and nonporous biodegradable polymeric hollow microspheres, J. Control. Release 35 (1995) 91-105.

[51] M. Sandor, D. Enscore, P. Weston, E. Mathiowitz, Effect of protein molecular weight on release from micron-sized PLGA microspheres, J Control. Release 76 (2001) 297-311.

[52] D.T. O'Hagan, H. Jeffery, S.S. Davis, The preparation and characterization of poly(lactide-co-glycolide) microparticles:III. Microparticle/polymer degradation rates and the in vitro release of a model protein, Int. J. Pharm. 103 (1994) 37-45.

[53] C. Sturesson, J. Carlfors, Incorporation of protein in PLG-microspheres with retention of bioactivity, J Control. Release 67 (2000) 171-178.

[54] J-M. Pean, M-C. Venier-Julienne, F. Boury, P. Menei, B. Denizot, J-P. Benoit, NGF release from poly(D,L-lactide-co-glycolide) microspheres. Effect of some formulation parameters on encapsulated NGF stability, J Control. Release 56 (1998) 175-187.

[55] W. Jiang and S.P. Schwendeman, Stabilization and controlled release of bovine serum albumin encapsulated in poly(D,L-lactide) and poly(ethylene glycol) microsphere blends, Pharm. Res. 18 (2001) 878-885.

[56] H.K. Kim, T.G. Park, Comparative study on sustained release of human growth hormone from semi-crystalline poly(L-lactic acid) and amorphous poly(D,L-lactic-co-glycolic acid) microspheres: morphological effect on protein release, J. Control. Release 98 (2004) 115-125.

[57] H.K. Sah, R. Toddywala and Y.W. Chien, The influence of biodegradable microcapsule formulations on the controlled release of a protein, J. Control. Release 30 (1994) 201-211.

[58] W. Friess and M. Schlapp, Modifiying the release of gentamicin from microparticles using a PLGA blend, Pharm. Dev. Technol. 7 (2002) 235-248.

[59] H.B. Ravivarapu, K. Burton, P.P. Deluca, Polymer and microsphere blending to alter the release of a peptide from PLGA microspheres, Eur. J. of Pharm. Biopharm. 50 (2000) 263-270.

[60] W. Wang, Instability, stabilization, and formulation of liquid protein pharmaceuticals, Int. J. Pharm. 185 (1999) 129-188.

[61] M. van de Weert, W.E. Hennink, W. Jiskoot, Protein instability in poly(lactic-co-glycolic acid) microparticles, Pharm. Res. 17 (2000) 1159-1165.

[62] R. Krishnamurthy, J.A. Lumpkin and R. Sridlar, Inactivation of lysozyme by sonication under conditions relevant to microencapsulation, Int. J. Pharm. 205 (2000) 23-34.

[63] H. Sah, Protein behaviour at the water/methylene chloride interface, J. Pharm. Sci. 88 (1999) 1320-1325.

[64] C.P. Rodriguez, N. Montano, K. Gonzalez, K. Griebenow, Stabilization of α-chymotrypsin at the CH_2Cl_2 / water interface and upon water-in-oil-in-water encapsulation in PLGA microspheres, J. Control. Release 89 (2003) 71-85.

[65] J.M. Pean, F. Boury, M.C. Vernier-Julienne, P. Menei, J.E. Proust, J.P. Benoit, Why does PEG 400 Co-encapsulation improve NGF stability and release from PLGA biodegradable microspheres? Pharm. Res. 16 (1999) 1294-1299.

[66] T. Uchida, K. Shiosaki, Y. Nakada, K. Fukada, Y. Eda, S. Tokiyoshi, N. Nagareya and K. Matsuyama, Microencapsulation of hepatitis B core antigen for vaccine preparation, Pharm. Res. 15 (1998) 1708-1713.

[67] T.G. Park, W. Lu, G. Crotts, Importance of in vitro experimental conditions on protein release kinetics, stability and polymer degradation in protein encapsulated poly(D,L-lactic acid-co-glycolic acid) microspheres, J Control. Release 33 (1995) 211-222.

[68] G. Zhu, S.R. Mallery, S.P. Schwenderman, Stabilization of proteins encapsulated in injectable poly(lactide-co-glycolide), Nature Biotech. 18 (2000) 52-57.

[69] M.A. Tracy, K.L. Ward, L. Firouzabadian, Y. Wang, N. Dong, R. Qian, Y. Zhang, Factors affecting the degradation rate of poly(lactide-co-glycolide) in vivo and in vitro, Biomaterials 20 (1999) 1057-1062.

[70] C. Yan, J.J. Resau, J. Heweston, M. West, W.L. Rill, M. Kende, Characterization and morphological analysis of protein-loaded poly(lactide-co-glycolide) microparticles prepared by water-in-oil-in-water emulsion technique, J Control. Release 32 (1994) 231-241.

[71] P.K. Smith, R.I. Krohn, G.T. Hermanson, A.K. Mallia, F.H. Gartner, M.D.

Provenzano, et al, Measurement of protein using bicinchroninic acid, Anal. Biochem. 150 (1985) 76-85.

[72] E.P. Magre and A.P. Sam, Hydrolytic degradation of PLAGA, calculation of rate constants from various types of in vitro degradation curves, J Control. Release 48 (1997) 318-319.

[73] S.T. Dillon and L.A. Feig, Purification and assay of recombinant C3 transferase, Methods Enzymol. 256 (1995) 174-184.

[74] M. Narito, S. Narumiya, Preparation of native and recombinant Clostridium botulinum C3 ADP-ribosyltransferase and identification of Rho proteins by ADP-ribosylation, Methods Enzymol. 256 (1995) 96-206.

[75] X.M. Lam, E.T. Duenas, A.L. Daugherty, N. Levin, J.L. Cleland, Sustained release of recombinant human insulin-like growth factor-I for treatment of diabetes, J. Control. Release 67 (2000) 281-292.

[76] C.G. Pitt, M.M Gratzl, G.L. Kimmel, J. Surles and A. Schindler, Aliphatic polyesters II. The degradation of poly(DL-lactide), poly(epsilon-caprolactone) and their copolymers in vivo, Biomaterials 2 (1981) 215-220.

[77] W.I. Li, K.W. Anderson, P.P. Deluca, Prediction of solvent removal profile and effect on properties for peptide-loaded PLGA microspheres prepared by solvent extraction/evaporation method, J. Control. Release 37 (1995) 199-214.

[78] J.L. Cleland, A.J.S. Jones, Stable formulations of recombinant human growth hormone and interferon-γ for microencapsulation in biodegradable microspheres, Pharm. Res. 13 (1996) 1464-1475.

[79] M. Wolf, M. Wirth, F. Pittner, F. Gabor, Stabilization and determination of the biological activity of L-asparaginase in poly(D,L-lactide-co-glycolide) nanospheres, Int. J. Pharm. 256 (2003) 141-152.

[80] A.A. Pouessel, M.C. Vernier-Julienne, A. Claveul, M. Sergent, C. Jollivet, N. C.N. Montero-Menei, et al., In vitro study of GDNF release from biodegradable PLGA microspheres, J. Control. Release 95 (2004) 463-475.

[81] J. Yang, J.L. Cleland, Factors affecting the in vitro release of recombinant human interferon-γ (rhIFN-γ) from PLGA microspheres, J. Pharm. Sc. 86 (1997) 908-914.

[82] H. Sah, Protein instability toward organic solvent/water emulsification: Implications for protein microencapsulation into microspheres, PDA J. Pharm. Sci. Technol. 53 (1999) 3-10.

[83] I.J. Castellanos, R. Crespo, K. Griebenow, Poly(ethylene glycol) as stabilizer and emulsifying agent: a novel stabilization approach preventing aggregation and inactivation of proteins upon encapsulation in bioerodible polyester microspheres, J. Control. Release 88 (2003) 135-145.

[84] S.P. Schwendeman, M. Cardamone, M.R. Brandon, A. Kilbanov, R. Langer, Stability of proteins and their delivery from biodegradable polymer microspheres, in S.Cohen, H. Bernstein (Eds.), Microparticulate systems for the delivery of proteins and vaccines, Marcel Dekker, New York, 1996.

[85] S.C. Piscitelli, W.G. Reiss, W.D. Figg, W.P. Petros, Pharmacokinetic studies with recombinant cytokines, scientific issues and practical considerations, Clin. Pharmacokinet. 32 (1997) 368-381.

[86] A. Sanchez, M. Tobio, L. Gonzalez, A. Fabra, M.J. Alonso, Biodegradable micro- and nanoparticles as long-term delivery vehicles for interferon-alpha, Eur. J. of Pharm. Sc. 18 (2003) 221-229.

[87] L. Chen, R.N. Apte, S. Cohen, Characterization of PLGA microspheres for the controlled delivery of IL-1α for tumor immunotherapy, J. Control. Release 43 (1997) 261-272.